PREDICTING CHEMICAL UPTAKE INTO SKIN

Richard H. Guy

University of Bath

Acknowledgements: Christophe Herkenne, Yogeshvar Kalia, Aarti Naik, Jonathan Hadgraft, Annette Bunge, Rodrigo Contreras-Rojas, Brian Saar, Sunney Xie, Natalie Belsey, Julian Moger, Natalie Garrett, Gareth Price, Hisamitsu Pharmaceutical Co. Ltd., Leo Pharma A/S.

Introduction

- **Drug delivery into and through skin for**
  - **dermatological therapy,**
  - **treatment of local, subcutaneous inflammation, or**
  - **to alleviate systemic disease,**

  continues to represent a major challenge.

- **While skin barrier function is better understood, and novel technologies are in development…**

  the problem of poor bioavailability remains.

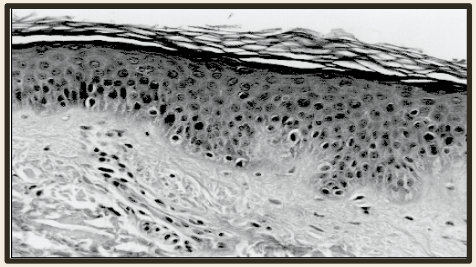

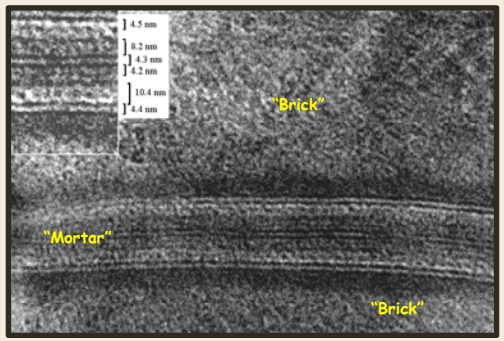

What is the value of being able to predict chemical uptake into skin?

- **Scheuplein & Blank first quantified rate and extent of skin absorption of diverse chemicals ➔ considerable effort to establishing relationships between molecular properties and skin permeation.**
- **Example objectives include:**
  - **identification/screening of potential drug candidates for (trans)dermal delivery**
  - **assessment of potential risk following dermal exposure to hazardous chemicals, such as pesticides**

Scheuplein, R.J., Blank, I.H., Brauner, G.J., MacFarlane, D.J., 1969. Percutaneous absorption of steroids. J. Invest. Dermatol. 52, 63-70.

Scheuplein, R.J., Blank, I.H., 1971. Permeability of the skin. Physiol. Rev. 51, 702-747.

Scheuplein, R.J., Blank, I.H., 1973. Mechanism of percutaneous absorption. IV. Penetration of nonelectrolytes (alcohols) from aqueous solutions and from pure liquids. J. Invest. Dermatol. 60, 286-296.

Scheuplein, R.J., 1976. Percutaneous absorption after twenty-five years: or "old wine in new wineskins". J. Invest. Dermatol. 67, 31-38.

Criteria for useful, quantitative "structure-penetration" relationships

- **Mechanistic insight consistent with, and validated against, skin barrier function and skin absorption experiments**
- **Predicts parameters suitable for its intended use (e.g., permeability coefficient, (trans)dermal flux, exposure)**
- **Comprehensible to scientists with "ordinary skill in the art"**
- **Model descriptors required are easily calculable or readily available in publicly-accessible sources**
- **Applicable across diverse chemical classes, not specific to a limited group of structurally-related compounds**
- **Modification (i.e., additional complexity) passes test of Ockham's Razor and can be justified statistically**

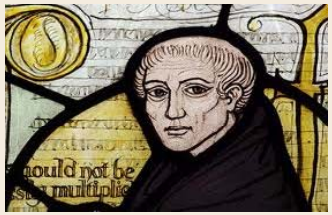

Key questions

- What are the key parameters and the physical rules that govern the rate and extent to which a chemical is taken up into the skin?
  - a solubility-diffusion problem
  - “Lipinski’s rules” for skin?
- How can skin uptake experiments be designed and interpreted to provide new predictive insight?
  - low-tech tape-stripping
  - high-tech Raman imaging

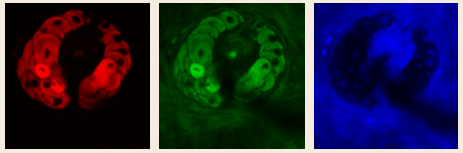

Rate and extent of chemical uptake into and absorption through the skin

- "Topical bioavailability"
- Approaches: in vitro, in silico, in vivo
- In vitro
  - Methodology and data analysis
  - Permeability coefficient, % dose absorbed
- In silico
  - Permeability coefficient
  - Maximum flux calculation
- In vivo
  - Stratum corneum tape-stripping {dermatopharmacokinetics, DPK}
  - Novel imaging approach based on Raman scattering microscopy (CARS/SRS)

$$\log K_p = -2.7 + 0.71 * \log P - 0.0061 * MW$$

Estimation of J_{max}

- **The absorption of a chemical into the skin depends upon:**
  - **its physicochemical properties**
  - **its presentation to the skin (i.e., the 'vehicle' in which it is applied)**
  - **the 'skin environment', and**
  - **the duration of exposure.**

- **Objectives:**
  - **to quantify the maximum absorbability of a chemical**
  - **to then evaluate exposure based upon the specific scenario involved**
    - **e.g., short-term versus long-term contact, infinite versus finite doses**

Theoretical development

- **Maximum flux (J_{max}), at which a chemical can cross a unit area of skin, is theoretically achieved when it is maintained as a saturated solution (or in neat chemical form) on the surface.**
- **Simple model applies Fick's 1st law:**
- $$J_{\max} = \frac{D}{\Delta x} * K_{\text{skin/vehicle}} * C^{\text{sat}}_{\text{vehicle}}$$

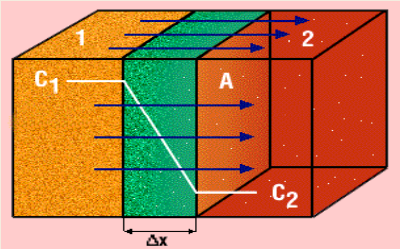

  - **D = chemical's diffusivity across skin (typically, stratum corneum)**
  - **Δx = diffusion path-length**
  - **$K_{skin/vehicle}$ = compound's partition coefficient between skin and vehicle,**
  - $C^{sat}_{vehicle}$ **= saturation solubility in vehicle.**
  - **Units of J are amount (e.g., moles or mg) per unit area per unit time.**

Theoretical development

If the vehicle is aqueous:

$$J_{max} = \frac{D}{\Delta x} * K_{skin/water} * C_{water}^{sat}$$

Define a permeability coefficient:

$$k_p = \frac{D}{\Delta x} * K_{skin/water}$$

Hence:

$$J_{max} = k_p * C_{water}^{sat}$$

Saturated aqueous solubilities are known, measurable or calculable

→ J_{max} can be determined if we can assess k_p

Theoretical development

Algorithm derived by Potts & Guy* from extensive database of ~100 K_p values across human skin in vitro following their application in water:

$$\log k_p = -2.7 + 0.71 * \log P - 0.0061 * MW$$

P = octanol-water partition coefficient of chemical

MW = molecular weight

Equation has reasonable predictive power

Units of k_p are cm/hr

Cleek & Bunge correction for highly lipophilic compounds:

$$k_p^{corr} = \frac{k_p}{1 + \frac{k_p \bullet \sqrt{MW}}{2.6}}$$

*R.O. Potts and R.H. Guy. Predicting skin permeability. *Pharm. Res.* 9, 663-669 (1992).

EDETOX database

http://www.ncl.ac.uk/edetox/theedetoxdatabase.html

In vitro absorption across human skin (n = 62)

log P: experimental, or ClogP

C_{sat}(aq): expt or calculated

Chemical Name	CAS	MW	LogP	log Kp	Kp (cm/h)	Csat (mg/cm3)	Jmax (mg/cm2/h)	Jmax (µg/cm2/h)
Methotrexate	59-05-2	454.45	-1.85	-6.786	1.63E-07	0.17	2.78E-08	0.00003
Benzo[a]pyrene	50-32-8	252.32	6.13	0.113	1.30E+00	1.14E-06	1.48E-06	0.00148
Aldosterone	52-39-1	360.44	1.08	-4.132	7.37E-05	0.05	3.68E-06	0.00368
Griseofulvin	126-07-8	352.77	2.18	-3.304	4.96E-04	8.66E-03	4.29E-06	0.00429
Acyclovir	59277-89-3	225.21	-1.56	-5.181	6.57E-06	1.62	1.06E-05	0.01065
Chlorpyrifos	2921-88-2	350.59	4.96	-1.317	4.82E-02	7.50E-04	3.61E-05	0.03613
T2 Toxin	21259-20-1	466.57	2.27	-3.934	1.16E-04	0.33	3.83E-05	0.03832
Cortisone	53-06-5	360.46	1.47	-3.855	1.39E-04	0.28	3.90E-05	0.03903
Hydrocortisone	50-23-7	362.47	1.61	-3.768	1.70E-04	0.39	6.64E-05	0.06644
Lindane	58-89-9	290.83	3.72	-1.833	1.47E-02	7.31E-03	1.07E-04	0.10733
Estradiol	50-28-2	272.37	4.01	-1.514	3.06E-02	3.60E-03	1.10E-04	0.11007
Methylene-Bis-(2-Chloroaniline)	101-14-4	267.00	3.91	-1.553	2.80E-02	4.62E-03	1.29E-04	0.12935
Dinitrochlorobenzene	97-00-7	202.55	2.17	-2.395	4.02E-03	0.037	1.49E-04	0.14891
Progesterone	57-83-0	314.45	3.87	-1.870	1.35E-02	1.17E-02	1.58E-04	0.15754
Testosterone	58-22-0	288.40	3.32	-2.102	7.90E-03	2.46E-02	1.94E-04	0.19432
Parathion	56-38-2	291.26	3.83	-1.757	1.75E-02	1.49E-02	2.60E-04	0.26031
Parathion methyl	298-00-0	263.21	2.86	-2.275	5.30E-03	5.50E-02	2.92E-04	0.29172
Diazinon	333-41-5	304.35	3.81	-1.851	1.41E-02	5.29E-02	7.44E-04	0.74420
Butachlor	23184-66-9	311.86	4.50	-1.407	3.91E-02	2.01E-02	7.86E-04	0.78631
Triclosan	3380-34-5	289.55	4.76	-1.087	8.19E-02	1.00E-02	8.19E-04	0.81875
Fluorouracil	51-21-8	130.08	-0.89	-4.125	7.48E-05	11.07	8.28E-04	0.82797
Mannitol	69-65-8	182.17	-2.20	-5.373	4.22E-06	220	9.29E-04	0.92943
Propranolol	525-66-6	257.34	3.48	-1.799	1.59E-02	6.17E-02	9.79E-04	0.97946
Nitro-1,4-Benzenediamine	5307-14-2	153.14	0.53	-3.258	5.52E-04	2.14	1.18E-03	1.18025
Cinnamyl anthranilate	87-29-6	253.30	4.74	-0.880	1.32E-01	1.10E-02	1.45E-03	1.45045
Methylenedianiline	101-77-9	198.27	1.59	-2.781	1.66E-03	0.99	1.64E-03	1.63903
Propoxur	114-26-1	209.25	1.52	-2.897	1.27E-03	1.86	2.35E-03	2.35378
Caffeine	58-08-2	194.20	-0.07	-3.934	1.16E-04	20.8	2.42E-03	2.41565
Pentachlorophenol	87-86-5	266.34	5.12	-0.689	2.04E-01	1.40E-02	2.86E-03	2.86108
Cinnamic acid	621-82-9	148.16	2.13	-2.091	8.09E-03	0.49	3.97E-03	3.96591
Coumarin	91-64-5	146.15	1.39	-2.605	2.48E-03	1.88	4.67E-03	4.66738
Acetylsalicylic Acid	50-78-2	180.16	1.19	-2.954	1.11E-03	4.42	4.91E-03	4.90698
DEET	134-62-3	191.28	2.18	-2.319	4.79E-03	1.62	7.76E-03	7.76406
Nicotinate benzyl	94-44-0	213.24	2.40	-2.297	5.04E-03	2.04	1.03E-02	10.29088
Nicotinic Acid	59-67-6	123.11	0.36	-3.195	6.37E-04	17.8	1.13E-02	11.33635
Nitrobenzene	98-95-3	123.11	1.85	-2.137	7.28E-03	1.95	1.42E-02	14.19641
Methyl-4-hydroxybenzoate	99-76-3	152.14	1.96	-2.236	5.80E-03	2.53	1.47E-02	14.66437
Urea	57-13-6	60.10	-2.11	-4.565	2.72E-05	550	1.50E-02	14.95651
Lidocaine	137-58-6	234.34	2.44	-2.397	4.00E-03	4.07	1.63E-02	16.29628
Cinnamyl alcohol	104-54-1	134.18	1.95	-2.134	7.34E-03	2.36	1.73E-02	17.31927
Phenylphenol	90-43-7	170.21	3.09	-1.544	2.85E-02	0.69	1.97E-02	19.68747
Salicylic acid	69-72-7	138.12	2.26	-1.938	1.15E-02	2.09	2.41E-02	24.09157
Benzoic Acid	65-85-0	122.10	1.87	-2.117	7.63E-03	3.44	2.62E-02	26.24623
Dimethylnitrosamine	62-75-9	74.08	-0.57	-3.557	2.77E-04	98.5	2.73E-02	27.30281
Benzene	71-43-2	78.12	2.13	-1.664	2.17E-02	1.79	3.88E-02	38.75713
Nicotinate hexyl	23597-82-2	207.27	3.51	-1.472	3.37E-02	1.43	4.82E-02	48.17522
Phenoxyethanol	122-99-6	138.17	1.16	-2.719	1.91E-03	26.9	5.13E-02	51.28913
Nicotinate methyl	93-60-7	137.14	0.83	-2.947	1.13E-03	47.6	5.37E-02	53.68116
Butoxyethanol	111-76-2	118.18	0.83	-2.832	1.47E-03	44.9	6.61E-02	66.09036
Safrole	94-59-7	162.19	3.45	-1.240	5.75E-02	1.24	7.13E-02	71.34101
Chloroform	67-66-3	119.38	1.97	-2.030	9.34E-03	8.07	7.53E-02	75.33379
Benzyl Alcohol	100-51-6	108.13	1.10	-2.579	2.64E-03	43.1	1.14E-01	113.61080
Nicotinate ethyl	614-18-6	151.17	1.32	-2.685	2.06E-03	56	1.16E-01	115.54927
Methoxypropan-2-ol	107-98-2	90.12	-0.49	-3.598	2.52E-04	470	1.19E-01	118.52209
Ethoxyethanol	110-80-5	90.12	-0.32	-3.477	3.33E-04	530	1.76E-01	176.48888
Nicotinate butyl	6938 06-3	129.22	2.27	-1.877	1.33E-02	18.35	2.44E-01	243.64412
Dimethylamine	124-40-3	45.10	-0.38	-3.245	5.68E-04	520	2.95E-01	295.46677
Phenol	108-95-2	94.11	1.46	-2.237	5.78E-03	94.1	5.44E-01	544.14601
Catechol	120-80-9	110.11	0.88	-2.747	1.79E-03	460	8.23E-01	822.98490
Dimethylethylamine	598-56-1	73.14	0.70	-2.649	2.24E-03	460	1.03E+00	1030.70071
Nicotine	54-11-5	162.23	1.17	-2.859	1.38E-03	1000	1.38E+00	1382.23488

EDETOX database

log P, MW and water solubility

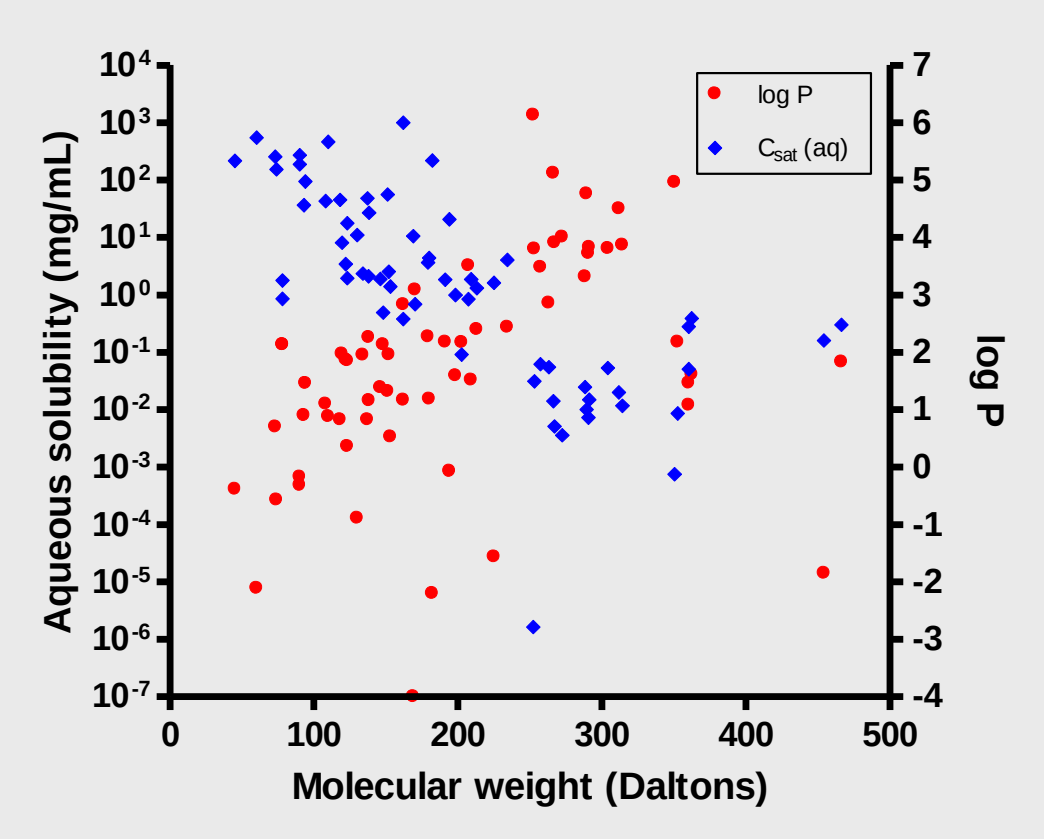

EDETOX database

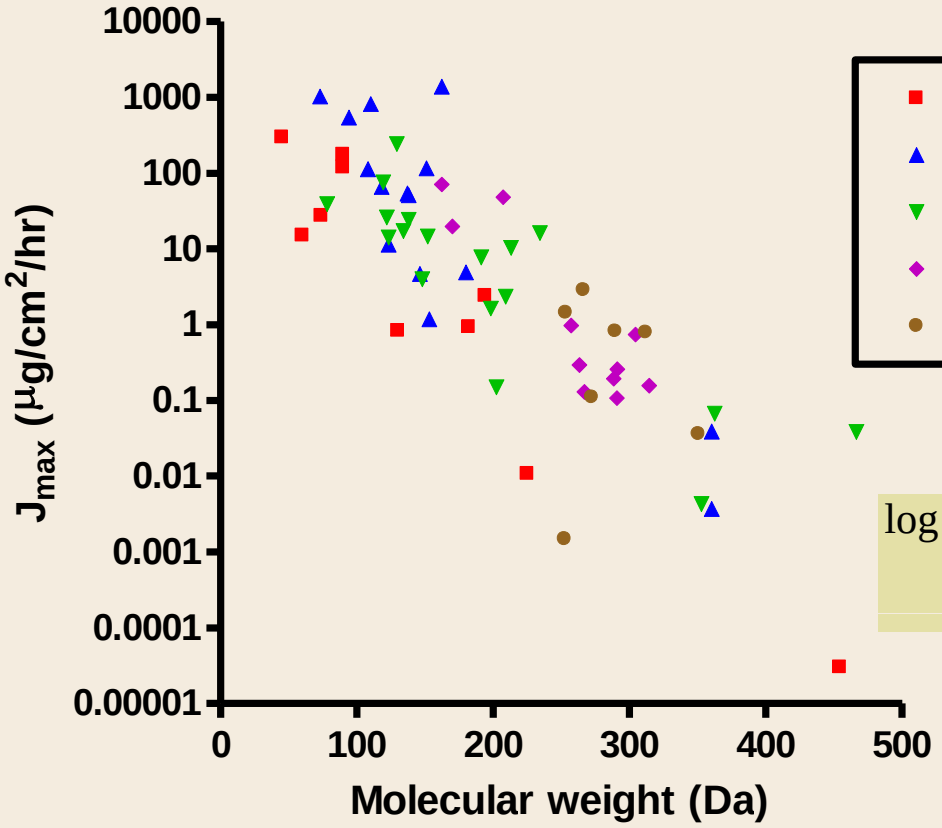

$$\log k_p = -2.7 + 0.71*\log P - 0.0061*MW$$

$$J_{max} = k_p * C_{water}^{sat}$$

EDETOX database

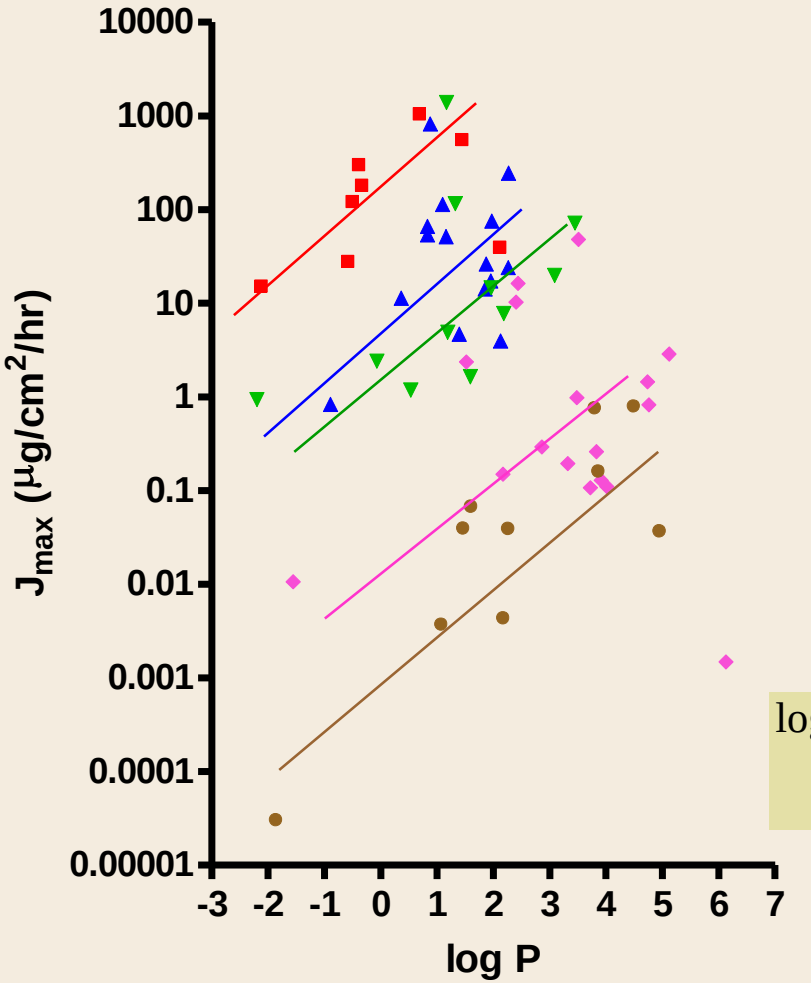

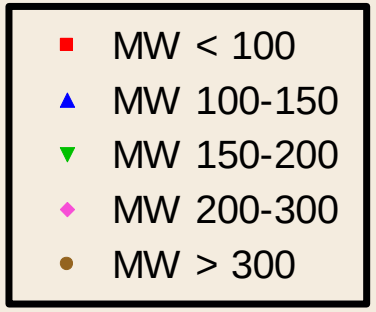

$$\log k_p = -2.7 + 0.71*\log P - 0.0061*MW$$

$$J_{max} = k_p * C_{water}^{sat}$$

Model validation: 14 compounds

Chemical Name	MW	log P	log kp	kp (cm/h)	kp,corr (cm/h)	Csat (mg/cm3)	Predicted Jmax (µg/cm2/h)	Experimental Jmax (µg/cm2/h)	Expt ÷ Prediction
Estradiol	272.4	4.01	-1.514	3.06E-02	2.56E-02	3.60E-03	0.09	0.031	0.34
Testosterone	288.4	3.32	-2.102	7.90E-03	7.51E-03	2.34E-02	0.18	0.22	1.25
Caffeine	194.2	-0.07	-3.934	1.16E-04	1.16E-04	21.6	2.51	6.65	2.65
Coumarin	146.2	1.39	-2.605	2.48E-03	2.45E-03	1.38	3.39	0.15	0.04
Nicotinate benzyl	213.2	2.40	-2.297	5.04E-03	4.91E-03	1.07	5.25	13.4	2.55
Methyl-4-hydroxybenzoate	152.1	1.96	-2.236	5.80E-03	5.64E-03	2.5	14.1	15.6	1.11
Salicylic acid	138.1	2.26	-1.938	1.15E-02	1.10E-02	2.24	24.5	26	1.06
Nicotinate butyl	179.2	2.27	-2.182	6.58E-03	6.36E-03	2.61	16.6	70	4.22
Nicotinate hexyl	207.3	3.51	-1.472	3.37E-02	2.84E-02	0.46	13.1	12.2	0.93
Nicotinate methyl	137.1	0.83	-2.947	1.13E-03	1.12E-03	47.6	53.4	240	4.49
Butoxyethanol	118.2	0.83	-2.832	1.47E-03	1.46E-03	44.9	65.7	66.9	1.02
Aniline	93.1	0.90	-2.629	2.35E-03	2.33E-03	36	83.7	218	2.61
Ethoxyethanol	90.1	-0.32	-3.477	3.33E-04	3.33E-04	539	179	44.5	0.25
Nicotinate ethyl	151.2	1.32	-2.685	2.06E-03	2.04E-03	56	114	260	2.27

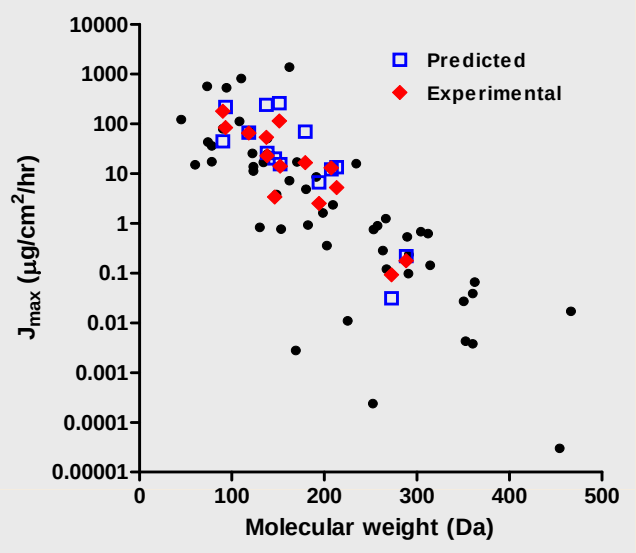

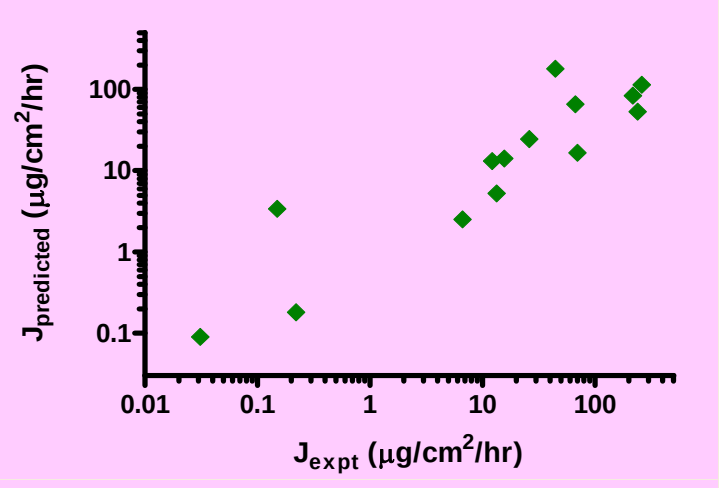

R.H. Guy. *Chem. Res. Toxicol.* 23 (2010) 864-870

Selected fragrance chemicals

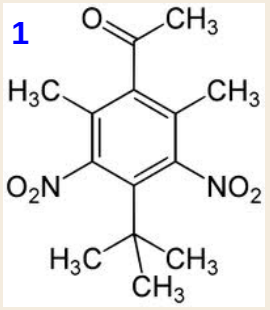

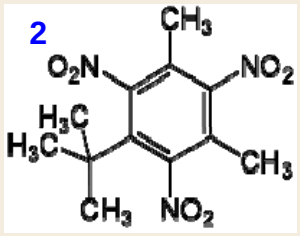

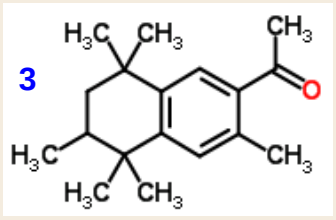

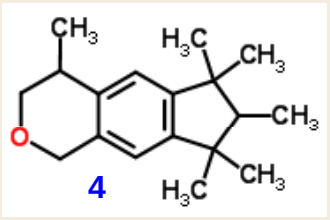

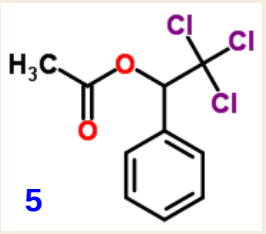

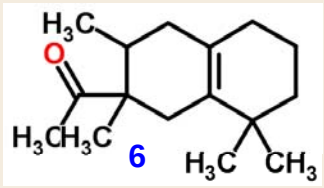

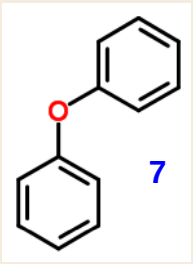

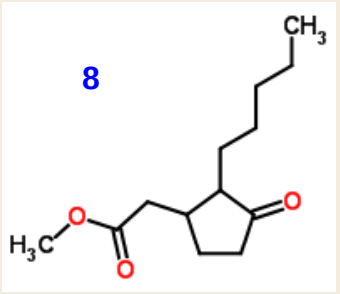

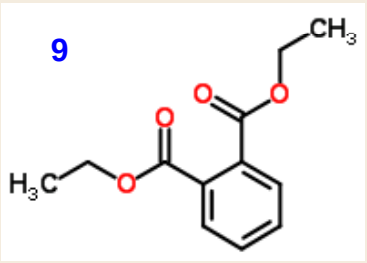

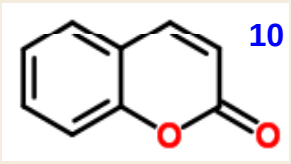

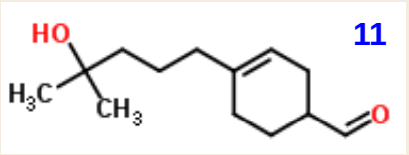

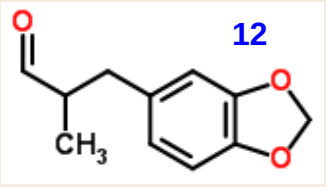

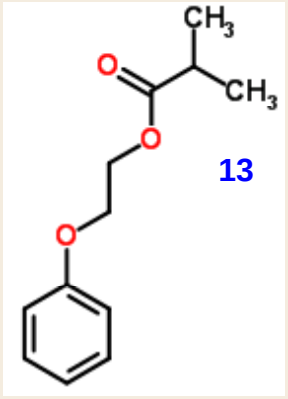

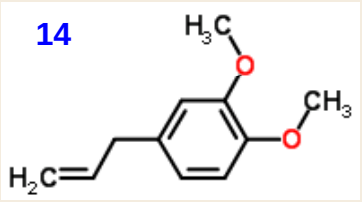

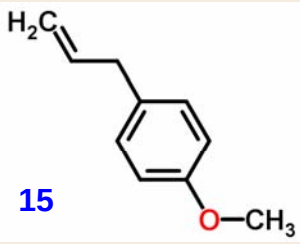

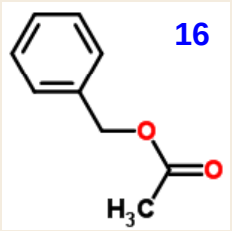

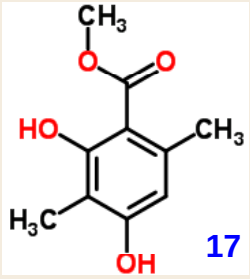

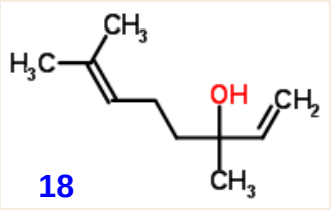

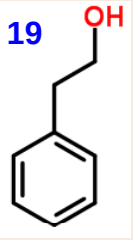

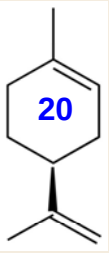

Chemical	MW	log P	$10^3 \cdot C_{sat,w}{}^a$ (mg/cm^3)	log k_P	k_P (cm/h)	$k_{P,corr}$ (cm/h)	J_{max} (µg/cm^2/h)
Musk ketone [1]	294.3	3.79 ± 0.40	4.1, 4.3, 1.9	-1.775	1.68E-02	1.51E-02	0.05
Musk xylene [2]	297.3	3.80 ± 0.29	4.6, 2.5, 7.1	-1.786	1.64E-02	1.48E-02	0.07
AHTN [3]	258.4	5.19 ± 0.66	0.65, 1.6, 2.0	-0.566	2.72E-01	1.01E-01	0.14
HHCB [4]	258.4	4.87 ± 0.82	0.8, 5.9, 2.1	-0.793	1.61E-01	8.07E-02	0.24
TPCA [5]	267.5	3.61 ± 0.26	8.0, 180, 79	-1.742	1.81E-02	1.63E-02	1.45
OTNE [6]	234.4	4.02 ± 0.59	32, 66, 19	-1.252	5.59E-02	4.21E-02	1.64
Diphenyl ether [7]	170.2	*4.21*	44, 21, 9.6	-0.732	1.85E-01	9.60E-02	2.37
Methyl dihydrojasmonate [8]	226.3	2.78 ± 0.32	120, 350, 440	-2.084	8.23E-03	7.86E-03	2.38
Diethyl phthalate [9]	222.2	*2.42*	380, 710, 630	-2.315	4.84E-03	4.71E-03	2.70
Coumarin [10]	146.2	*1.33*	1000, 620, 1600	-2.590	2.57E-03	2.54E-03	2.72
HMPCC [11]	210.3	2.61 ± 0.47	310, 420, 460	-2.109	7.78E-03	7.46E-03	2.96
MMDHCA [12]	192.2	2.18 ± 0.35	320, 210, 1430	-2.305	4.95E-03	4.82E-03	3.15
2-phenoxyethyl isobutyrate [13]	208.3	2.74 ± 0.20	130, 1130, 710	-2.004	9.89E-03	9.38E-03	6.16
Methyl eugenol [14]	178.2	2.74 ± 0.26	190, 770, 550	-1.824	1.50E-02	1.39E-02	7.01
Estragole [15]	148.2	3.08 ± 0.30	75, 670, 460	-1.402	3.96E-02	3.34E-02	13.41
Benzyl acetate [16]	150.2	*1.96*	520, 1850, 5980	-2.210	6.17E-03	5.99E-03	16.68
Methyl atratate [17]	196.2	2.30 ± 0.46	2540, 2760, 4100	-2.244	5.69E-03	5.52E-03	17.31
Linalool [18]	154.3	*2.97*	480, 1090, 1940	-1.517	3.04E-02	2.65E-02	31.04
Phenylethyl alcohol [19]	122.2	*1.36*	11300, 2990, 25000	-2.468	3.40E-03	3.36E-03	43.91
d-limonene [20]	136.2	*4.57*	460, 390, 50	-0.273	5.34E-01	1.57E-01	47.13

R.H. Guy. *Chem. Res. Toxicol.* 23 (2010) 864-870

Chemical	kp,corr (cm/h)	Jmax (µg/cm2/h)	Qapp (µg)	A (cm2)	tapp (hr)	%DA pred.	%DA expt	%DA expt/pred	Jmax expt/pred	kp expt/pred
Musk ketone	1.51E-02	0.05	180	1	16	0.46	0.10	0.22		
Musk xylene	1.48E-02	0.07	3	1	24	56	1.0	0.02		
AHTN	1.01E-01	0.14	200	1	24	1.7	4.1	2.4		
AHTN	1.01E-01	0.14	1090	100	6	7.9	0.90	0.11		
HHCB	8.07E-02	0.24	200	1	24	2.8	0.38	0.14		
HHCB	8.07E-02	0.24	18	1	6	7.9	0.10	0.01		
TPCA	1.63E-02	1.45	5000	100	6	17.0	5.0	0.29		
OTNE	4.21E-02	1.64	198	1	48	40	15	0.38		
Methyl dehydrojasmonate	7.86E-03	2.38	200	1	48	57	46	0.81		
Diethyl phthalate	4.71E-03	2.70	18450	1	72	1.1	4.7	4.5	0.47	
Coumarin	2.54E-03	2.72	3.7	1	72	100	50	0.50		
HMPCC	7.46E-03	2.96	90.2	1.2	24	94	36	0.39		
MMDHCA	4.82E-03	3.15	198	1	48	76	50	0.66		
Methyl eugenol	1.39E-02	7.01	198.5	1	48	100	34	0.34		
Methyl eugenol	1.39E-02	7.01	640	0.64	24	17	9.0	0.53		
Estragole	3.34E-02	13.4	201	1	48	100	16	0.16		
Benzyl acetate	5.99E-03	16.7	4	1	24	100	78	0.78		
Methyl atratate	5.52E-03	17.3	200	1	48	100	20	0.20		
Phenylethyl alcohol	3.36E-03	43.9								8.67

Prediction of % dose absorbed

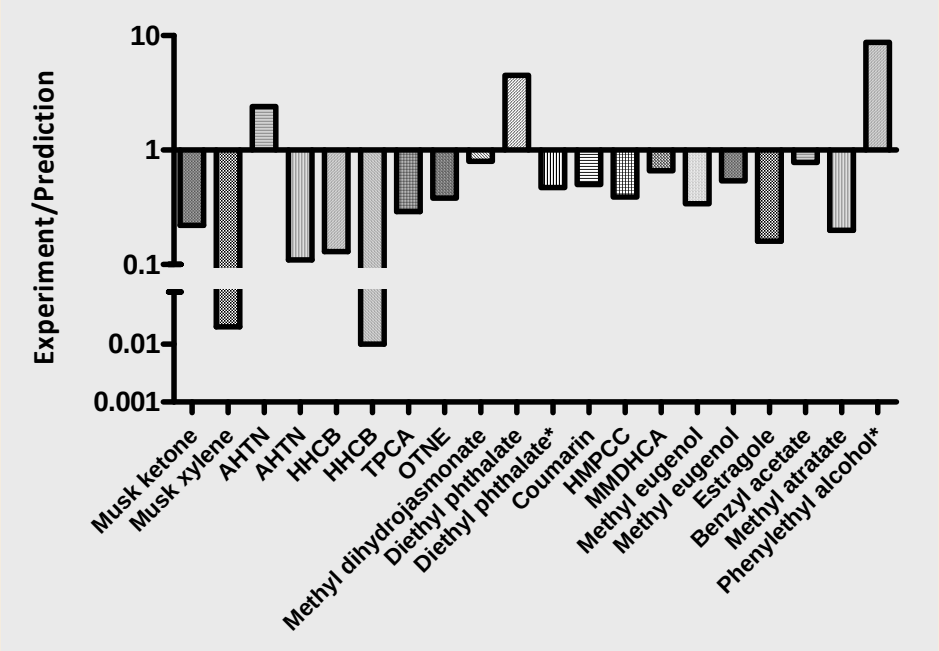

R.H. Guy. *Chem. Res. Toxicol.* 23 (2010) 864-870.

Predicting skin permeability of chemicals

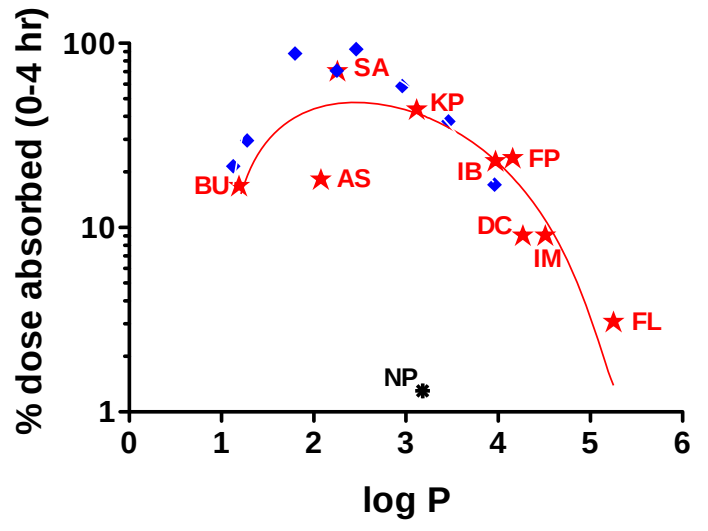

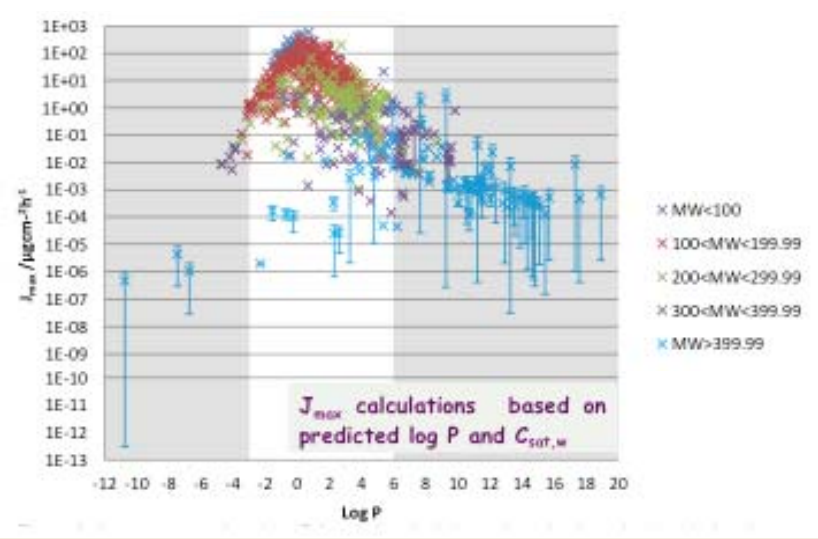

$$J_{\max} = k_p * C_{water}^{sat}$$

$$\log k_p = -2.7 + 0.71 * \log P - 0.0061 * MW$$

$$k_p^{corr} = \frac{k_p}{1 + \frac{k_p \bullet \sqrt{MW}}{2.6}}$$

Observations

- **Solubility-diffusion approach provides a decent "first-order" estimate of skin uptake.**
  - **Key parameters are (at least) MW, log P and (aqueous) solubility.**
- **Predictions validated for maximum flux and permeability coefficient; potential also for finite dose, short-contact scenarios.**
  - **Feasibility/success of (trans)dermal drug delivery depends, therefore, on both percutaneous penetration and pharmacological potency.**
  - **A Lipinsky-type set of rules is operative.**

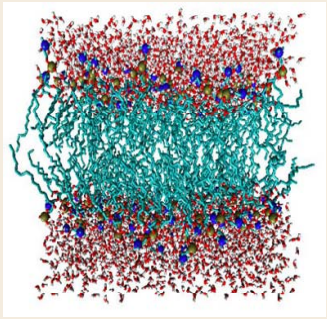

Key questions

- What are the key parameters and the physical rules that govern the rate and extent to which a chemical is taken up into the skin?
  - a solubility-diffusion problem
  - "Lipinski's rules" for skin?
- **How can skin uptake experiments be designed and interpreted to provide new predictive insight?**
  - **low-tech tape-stripping**
  - **high-tech Raman imaging**

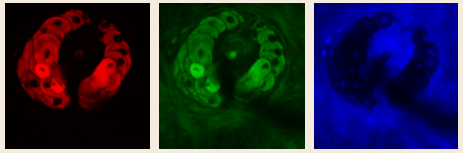

Assessing skin bioavailability *in vivo* in man

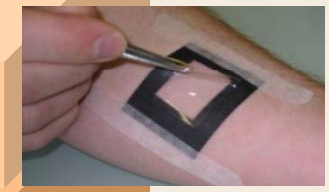

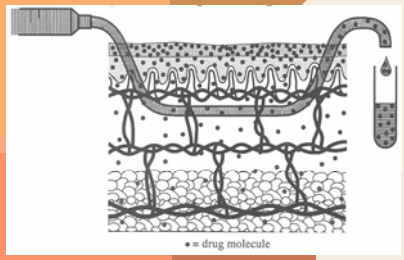

Stratum Corneum

Epidermis

Dermis

Pharmacodynamic assay

Tape-stripping

Suction blister X

Microdialysis

Biopsy X

Blood levels

Sampling the skin: tape-stripping

Determination of drug concentration in stratum corneum (SC) by sequential removal of thin layers of SC at same site with adhesive tape.

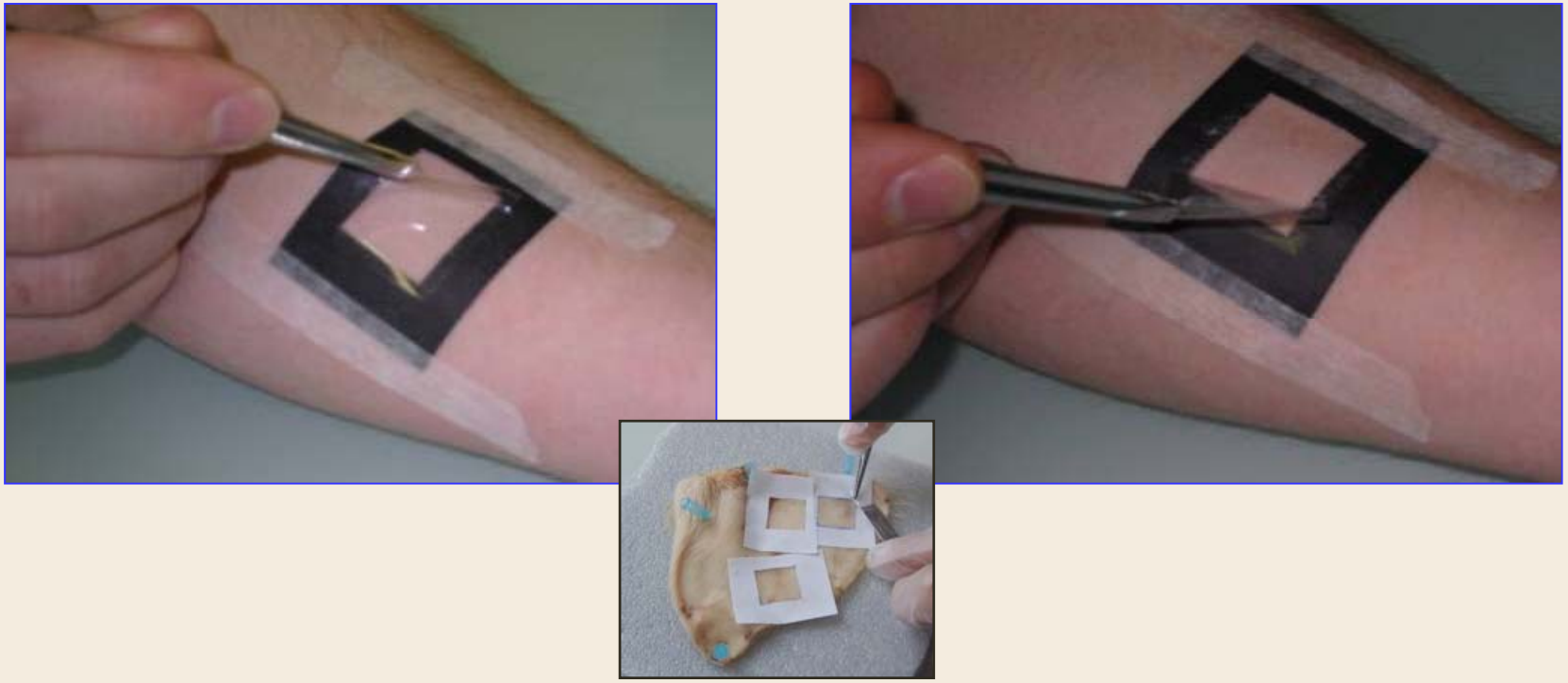

FDA proposal

- **Dermatopharmacokinetic (DPK) approach to replace clinical trials (primarily for bioequivalence).**
  - **determination of stratum corneum concentration-time curves for topical actives**
  - ***analogous to plasma/urine concentration-time curves for systemically administered drugs***

Assumption: SC concentration-time curves are directly related to concentration-time curves in the epidermis and dermis.

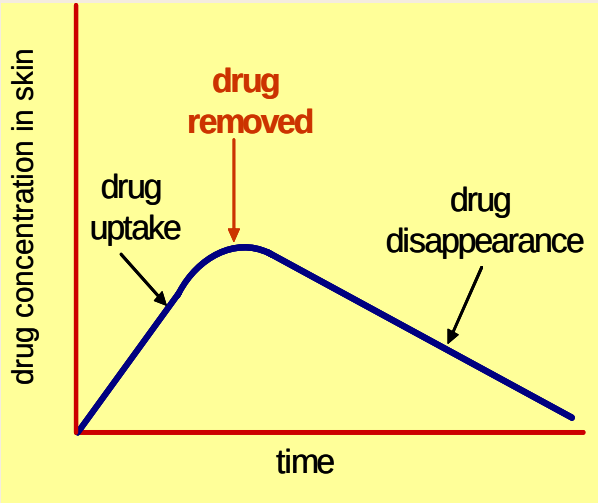

Distribution profile of active across the stratum corneum (SC)

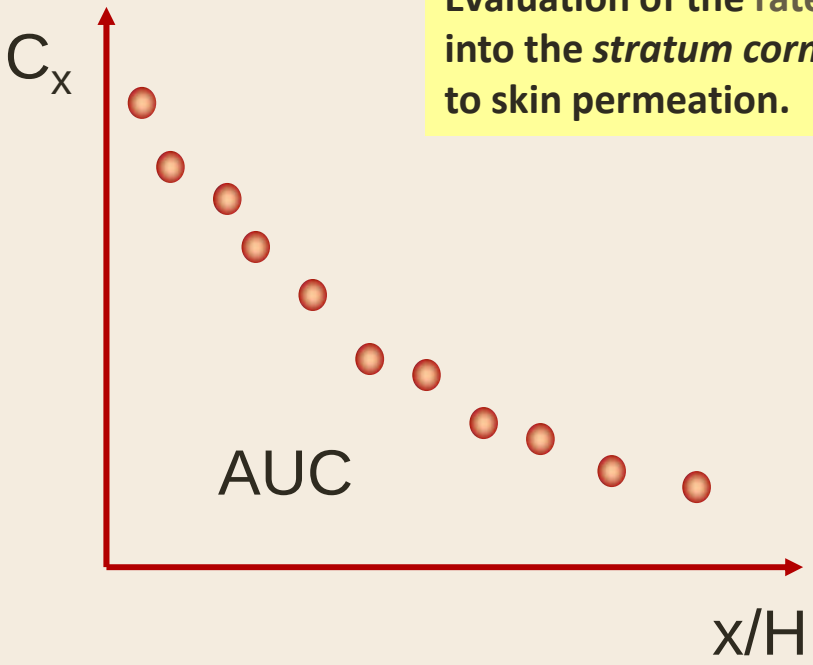

Evaluation of the rate and extent of active penetration into the *stratum corneum* - the rate-determining barrier to skin permeation.

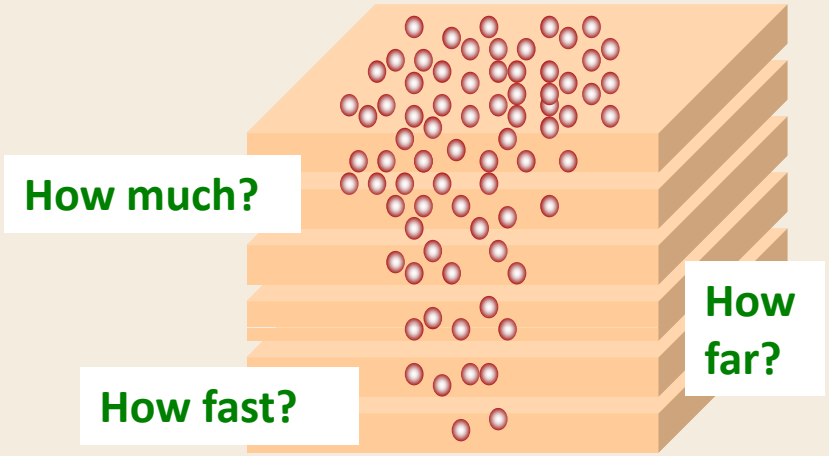

Measure active concentration profile as a function of position in the SC

Required: (i) amount on each strip, (ii) penetration depth into SC

Tape-stripping and barrier function

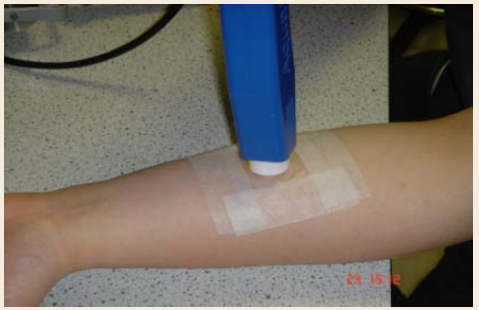

Transepidermal water loss (TEWL) increases 20-fold as the stratum corneum is removed

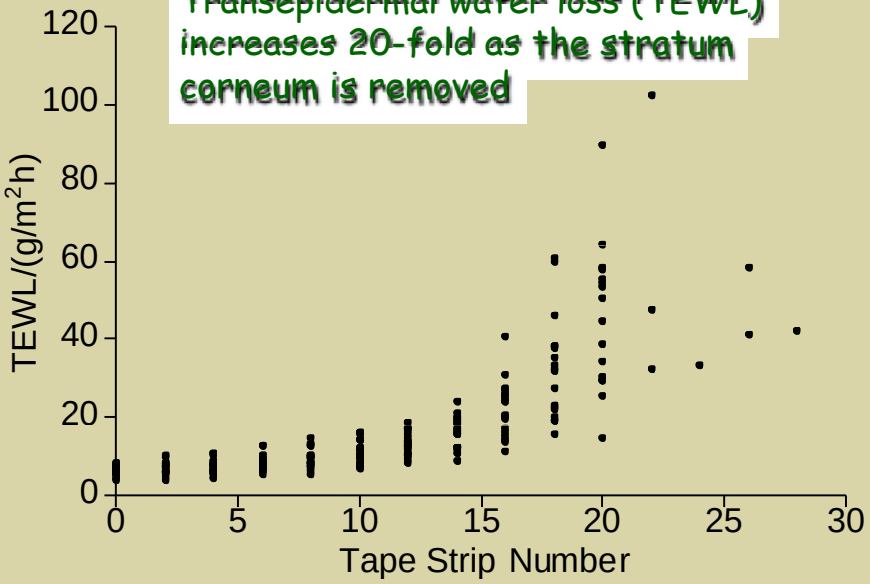

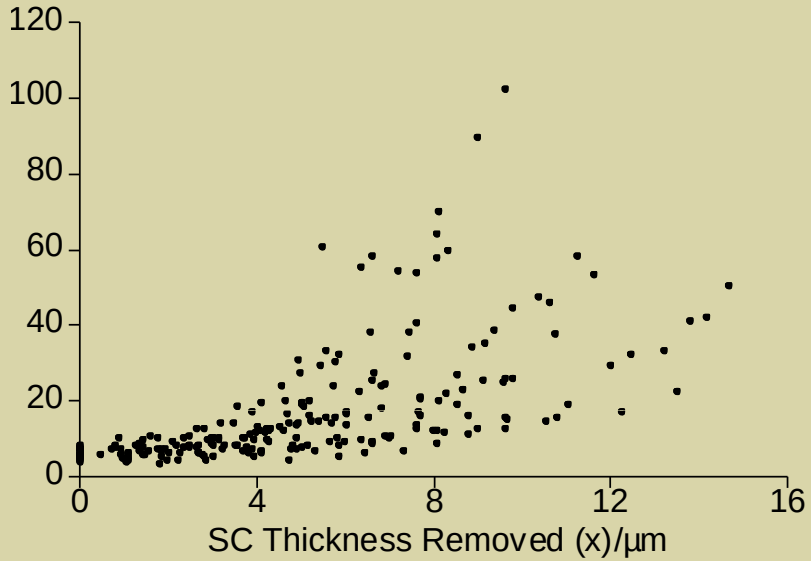

Tape-stripping removes different amounts of SC in different subjects

SC thickness varies between different subjects

Determination of SC thickness and depth

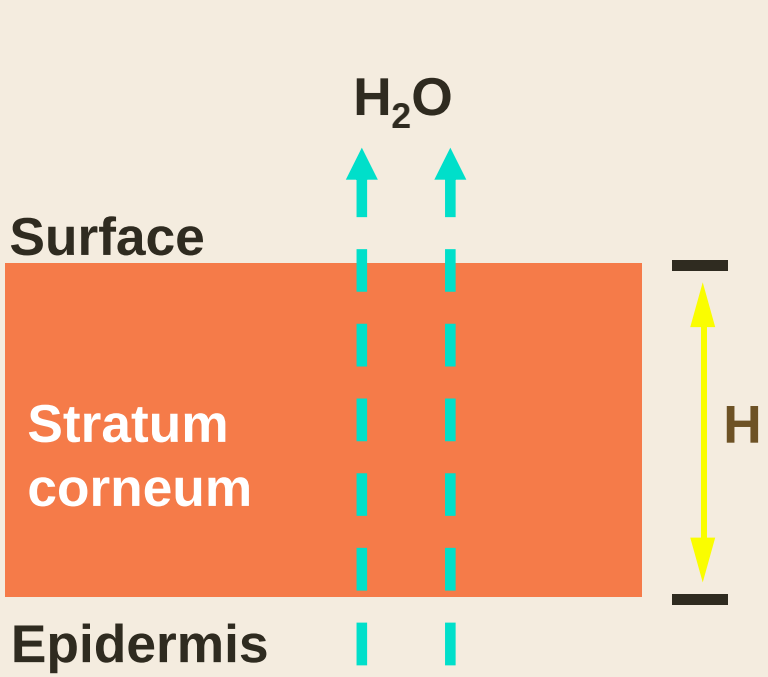

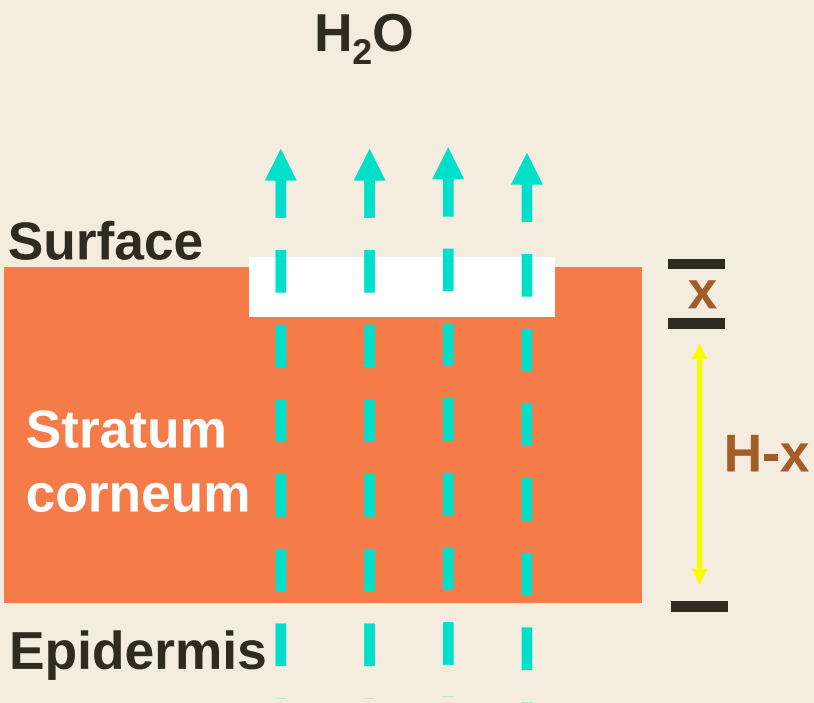

$$J_0 = TEWL_0 = \frac{K \bullet D}{H} \Delta C$$

$$J_x = TEWL_x = \frac{K \bullet D}{(H - x)} \Delta C$$

Determination of SC thickness

$$J_x = TEWL_x = \frac{K \bullet D}{(H - x)} \Delta C$$

$$\frac{1}{J} = \frac{1}{TEWL_x} = \frac{H}{D \cdot K \cdot \Delta C} - \frac{x}{D \cdot K \cdot \Delta C}$$

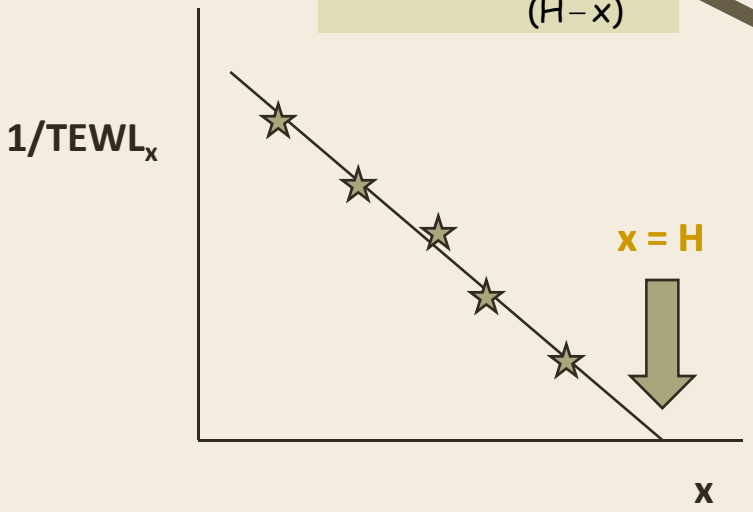

Plot $1/TEWL_x$ *versus* x and extrapolate to $1/TEWL_x = 0$

Intercept = H

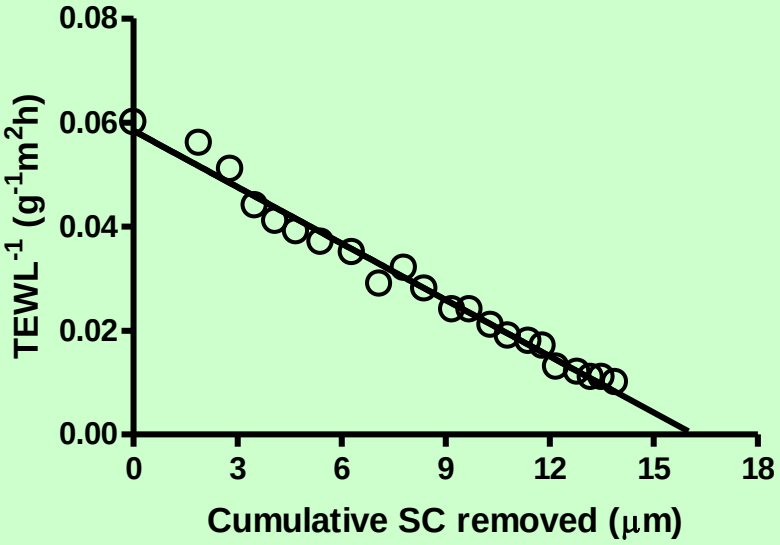

Tape-stripping and barrier function

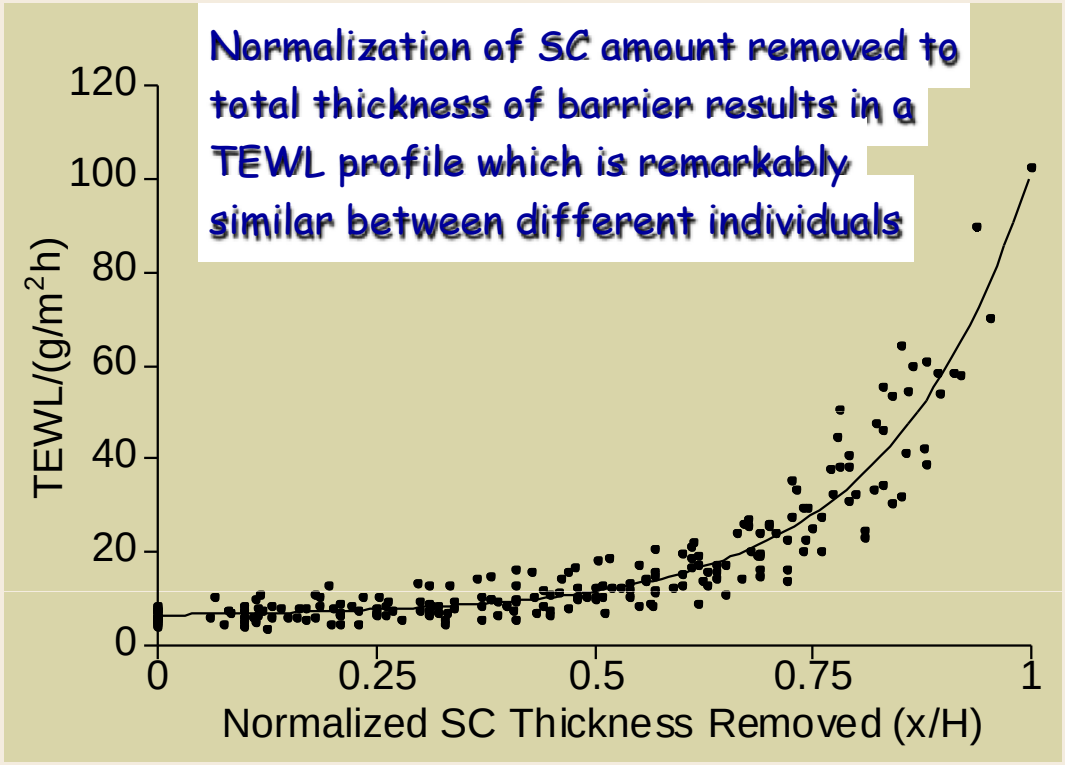

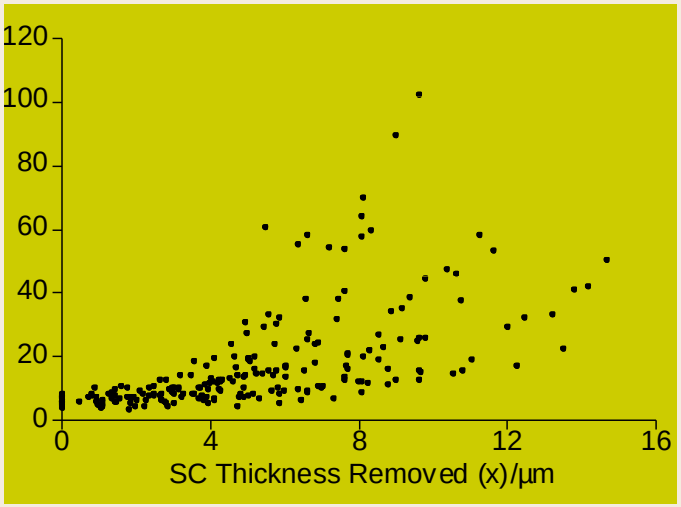

Y.N. Kalia, I. Alberti, N. Sekkat, C. Curdy, A. Naik and R.H. Guy. *Pharm. Res.* 17: 1148-1150 (2000).

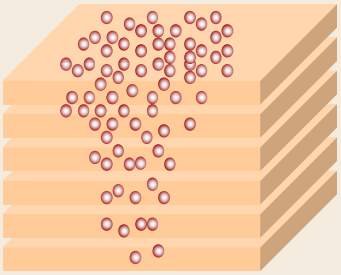

Drug concentration profile in the SC

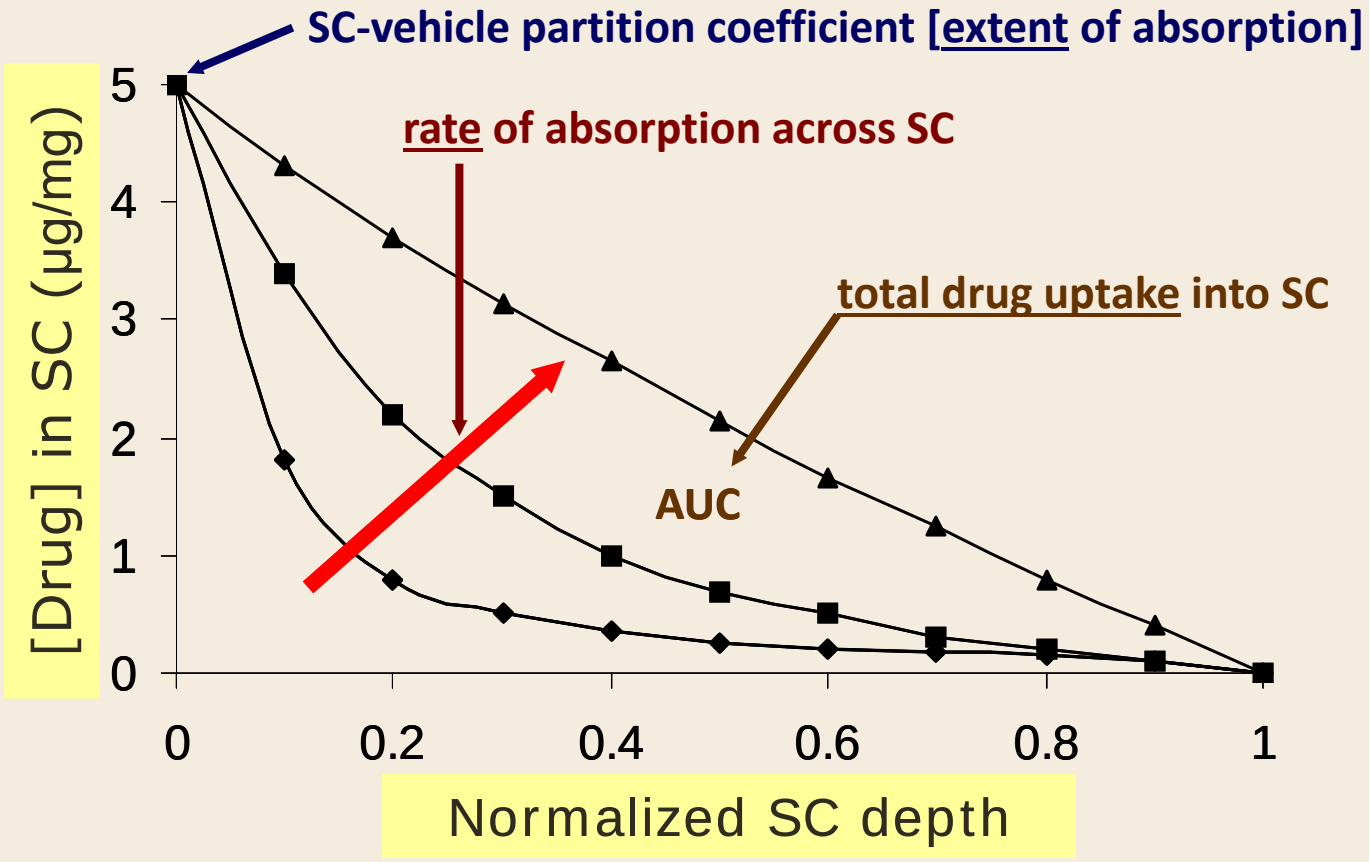

Drug concentration profile in the SC

$$\frac{\partial C}{\partial t} = D\frac{\partial\ C}{\partial x^2}$$

$$C_x = K \bullet C_{veh}\{1 - x/L - 2/\pi \sum_{n=1}^{\infty} 1/n \bullet \sin(n\pi x/L) \bullet \exp(-D/L^2 n^2 \pi^2 t)\}$$

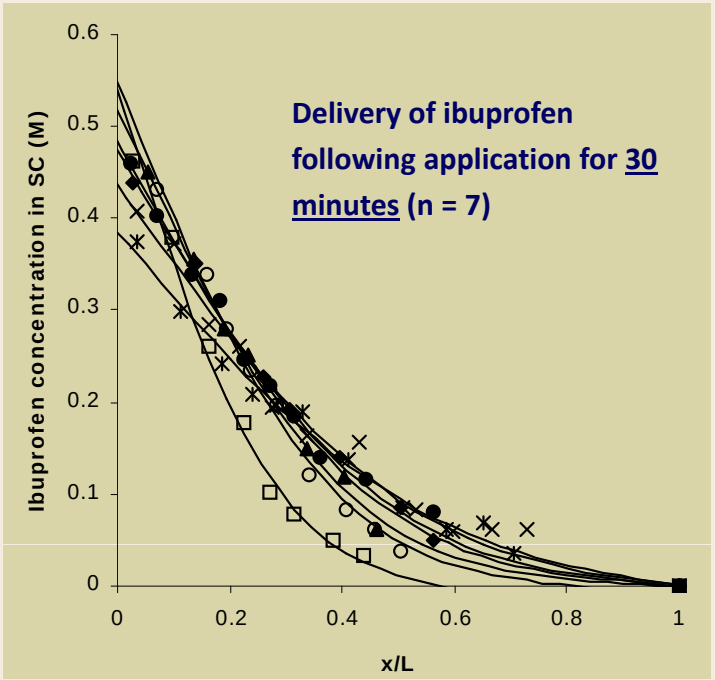

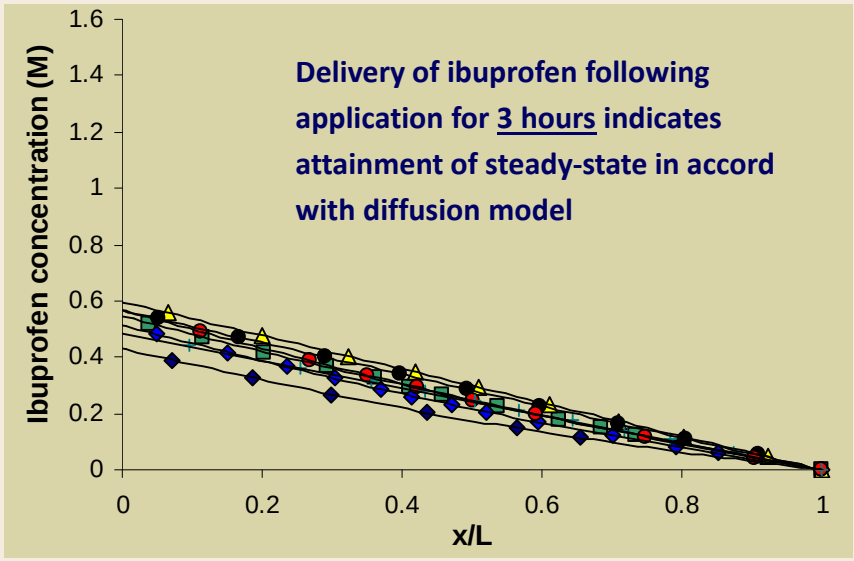

C. Herkenne, A. Naik, Y.N. Kalia, J. Hadgraft and R.H. Guy. *J. Pharm. Sci.*, 97, 185-197 (2008).

Terbinafine: effect of oleic acid

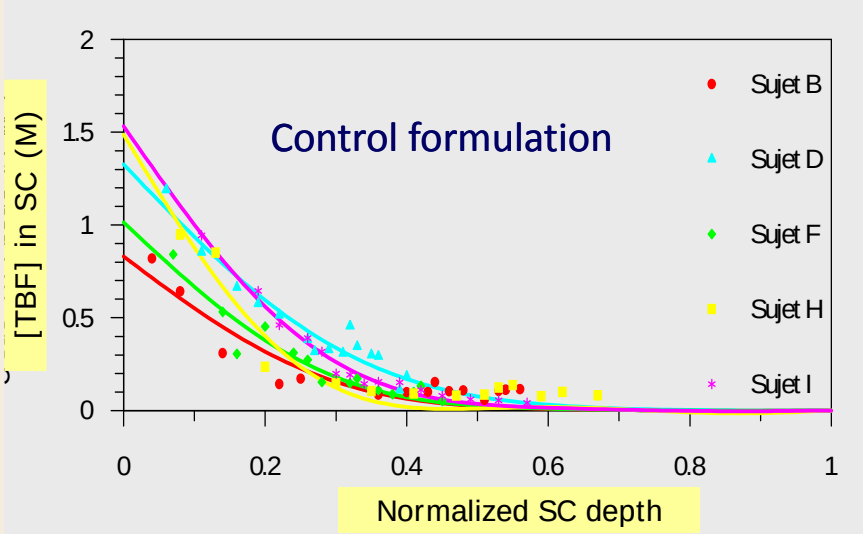

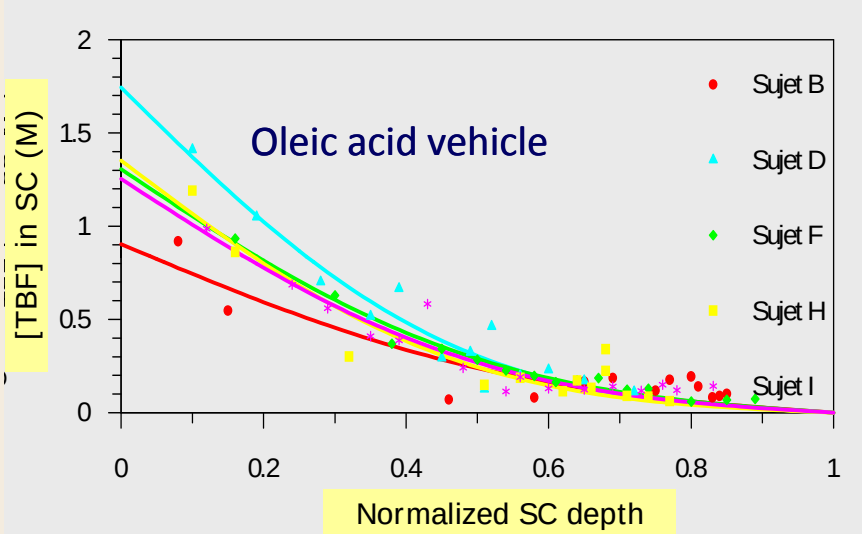

Formulation	K	$D/L^2 *10^6 (s^{-1})$
Control	0.70 ± 0.18	3.5 ± 0.9
Oleic acid	0.75 ± 0.17	12 ± 2.1*

*significantly different from control ($p < 0.05$)

I. Alberti, Y.N. Kalia, A. Naik, J.-D. Bonny and R.H. Guy. *J. Control. Release*, 71: 319-327 (2001).

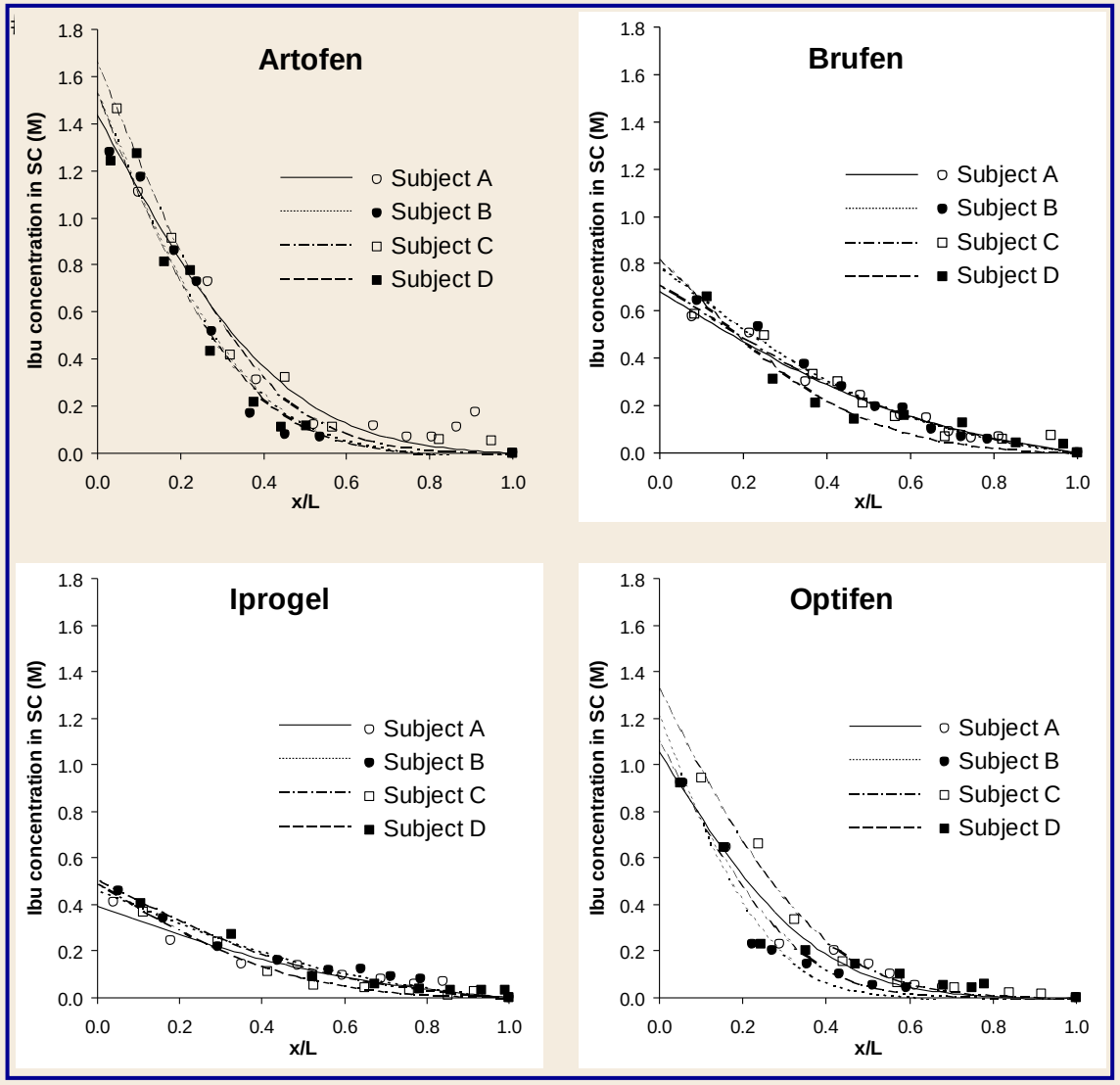

C. Herkenne et al., J. Invest. Dermatol. 127, 135-142 (2007)

Dermatopharmacokinetic evaluation of topical gel bioequivalence

4 commercial gel formulations of ibuprofen as a model active, enabling comparison and evaluation of:

- different formulations of supposedly equivalent efficacy
- different concentrations and manufacturers
- Artofen (10%), Brufen (5%), Iprogel (5%), Optifen (5%)

Formulation	K	D/L^2 [h^{-1}]	AUC (M)	Amount in SC (μg)	10^3*Kp [cm / h]	J_{ss} [μg cm^{-2} h^{-1}]
ARTOFEN	3.16 ± 0.19	0.095 ± 0.020	0.374 ± 0.035	482 ± 19	0.37 ± 0.04	37.1 ± 3.7
BRUFEN	3.11 ± 0.26	0.211 ± 0.054	0.264 ± 0.021	343 ± 47	0.81 ± 0.19	40.7 ± 9.7
IPROGEL	1.92 ± 0.21	0.211 ± 0.055	0.163 ± 0.018	212 ± 34	0.51 ± 0.14	25.4 ± 7.2
OPTIFEN	4.80 ± 0.47	0.072 ± 0.022	0.247 ± 0.051	317 ± 47	0.43 ± 0.13	21.4 ± 6.4

C. Herkenne et al., J. Invest. Dermatol. 127, 135-142 (2007)

Fitting of data following application for 30 minutes yields estimates of transport parameters:

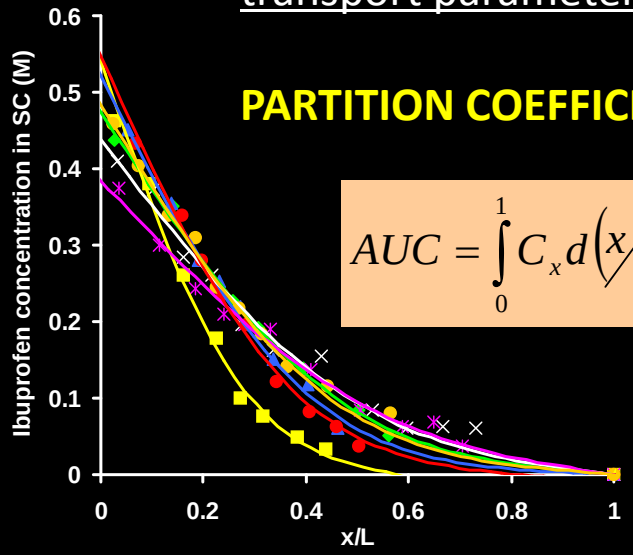

PARTITION COEFFICIENT, K

DIFFUSION PARAMETER, D/L^2

$$AUC = \int_0^1 C_x \, d\left(x/L\right) = K.C_v \left\{ \frac{1}{2} - \frac{4}{\pi^2} \sum_{n=0}^{\infty} \frac{1}{(2n+1)^2} \exp\left(- \frac{(2n+1)^2 . \pi^2 . D t}{L^2} \right) \right\}$$

Fitting of data following application for 30 minutes yields estimates of transport parameters:

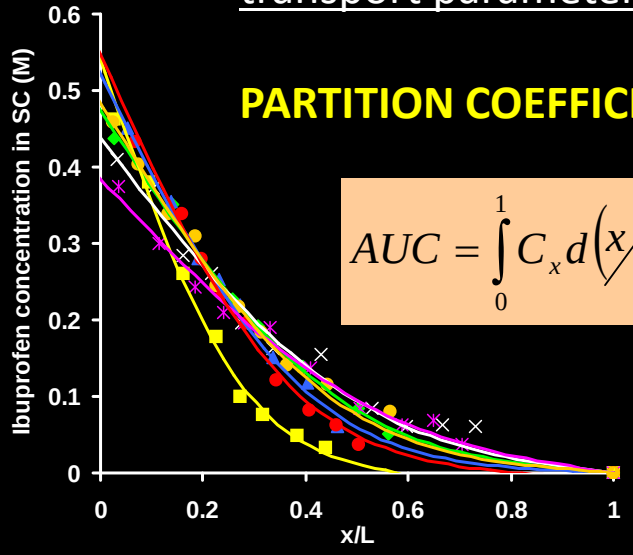

PARTITION COEFFICIENT, K

DIFFUSION PARAMETER, D/L^2

$$AUC = \int_0^1 C_x \, d\left(x/L\right) = K.C_v \left\{ \frac{1}{2} - \frac{4}{\pi^2} \sum_{n=0}^{\infty} \frac{1}{(2n+1)^2} \exp\left(- \frac{(2n+1)^2 . \pi^2 . D t}{L^2} \right) \right\}$$

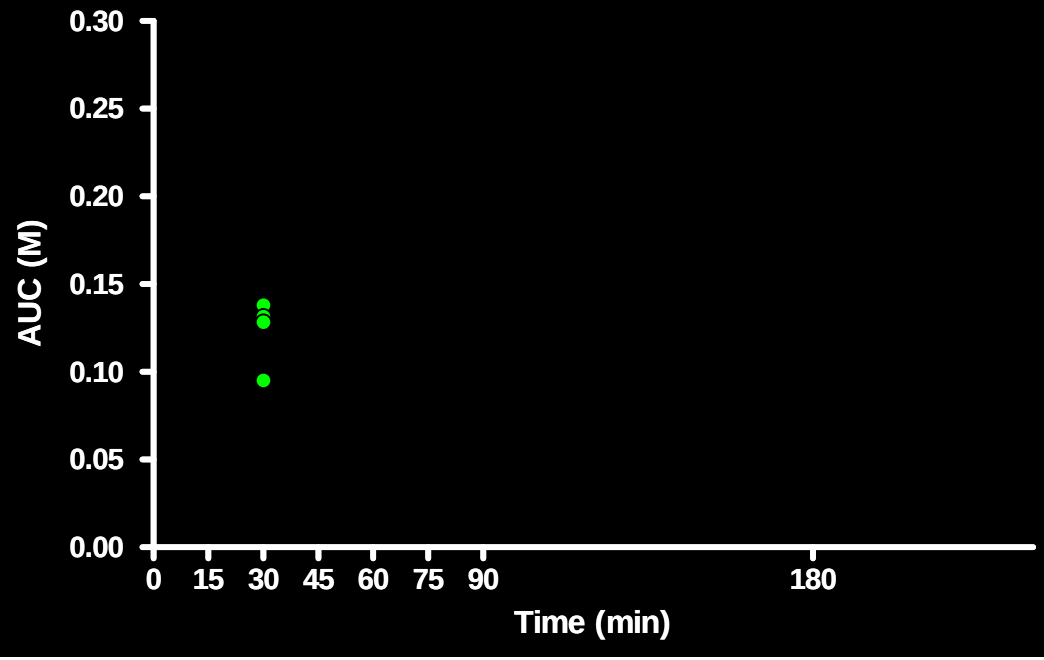

EXPERIMENTAL VALUES (n=7)

K = 2.8 ± 0.3

$D/L^2 = 0.12 \pm 0.05\ h^{-1}$

C. Herkenne et al., J. Invest. Dermatol., 127: 887-894(2007).

Fitting of data following application for 30 minutes yields estimates of transport parameters:

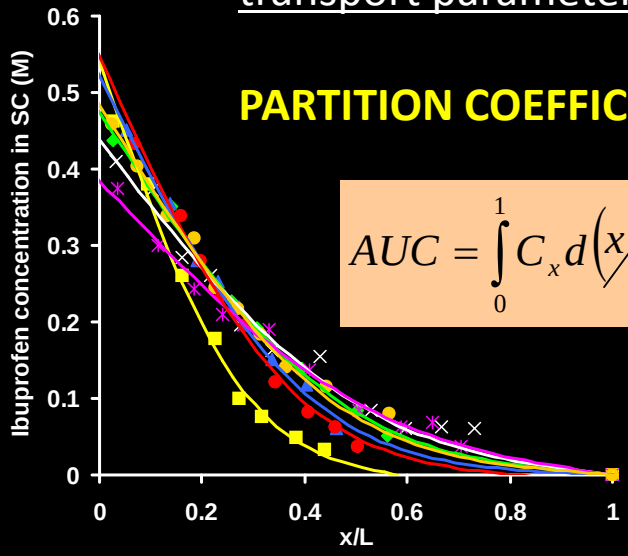

PARTITION COEFFICIENT, K

DIFFUSION PARAMETER, D/L^2

$$AUC = \int_0^1 C_x \, d\left(x/L\right) = K.C_v \left\{ \frac{1}{2} - \frac{4}{\pi^2} \sum_{n=0}^{\infty} \frac{1}{(2n+1)^2} \exp\left(- \frac{(2n+1)^2 . \pi^2 . D t}{L^2} \right) \right\}$$

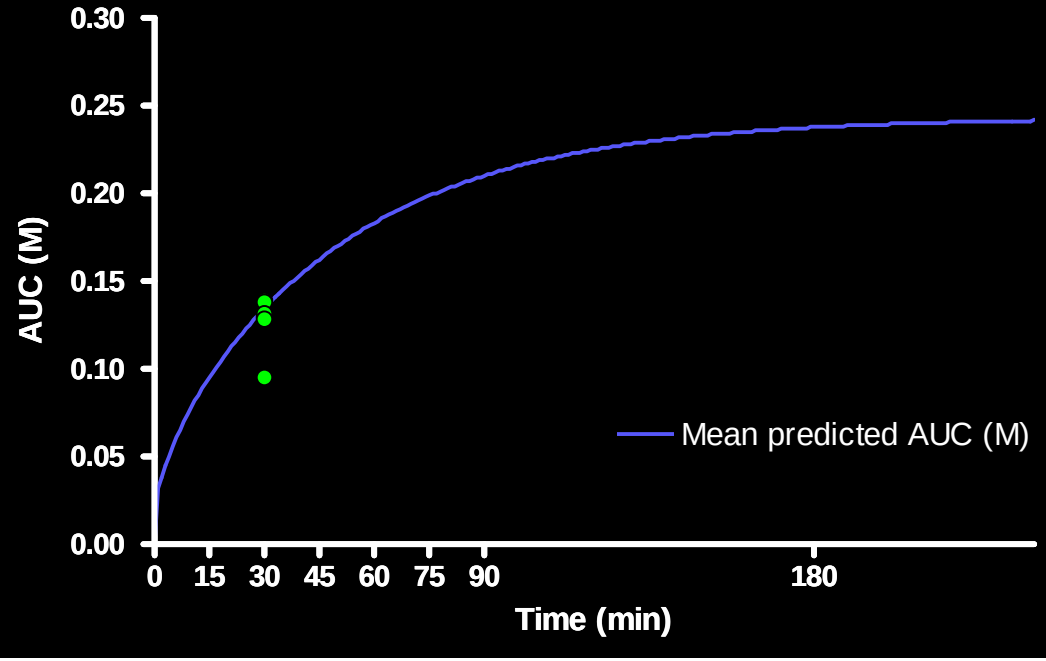

EXPERIMENTAL VALUES (n=7)

K = 2.8 ± 0.3

$D/L^2 = 0.12 \pm 0.05\ h^{-1}$

C. Herkenne et al., J. Invest. Dermatol., 127: 887-894(2007).

Fitting of data following application for 30 minutes yields estimates of transport parameters:

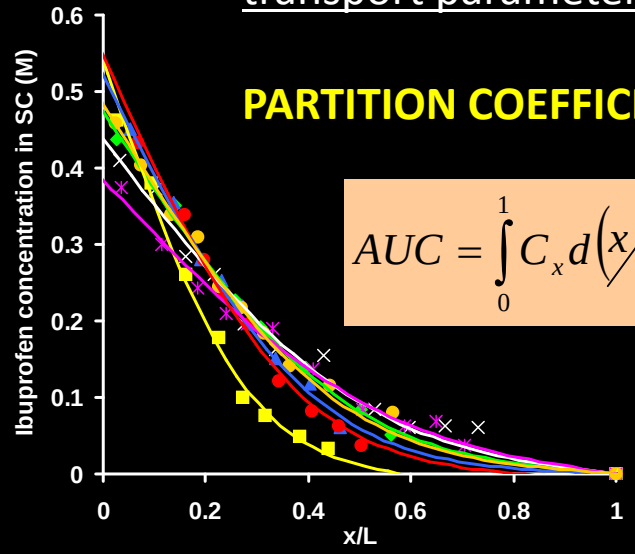

PARTITION COEFFICIENT, K

DIFFUSION PARAMETER, D/L^2

$$AUC = \int_0^1 C_x\, d\left(x/L\right) = K.C_v\left\{\frac{1}{2} - \frac{4}{\pi^2}\sum_{n=0}^{\infty}\frac{1}{(2n+1)^2}\exp\left(-\frac{(2n+1)^2.\pi^2.Dt}{L^2}\right)\right\}$$

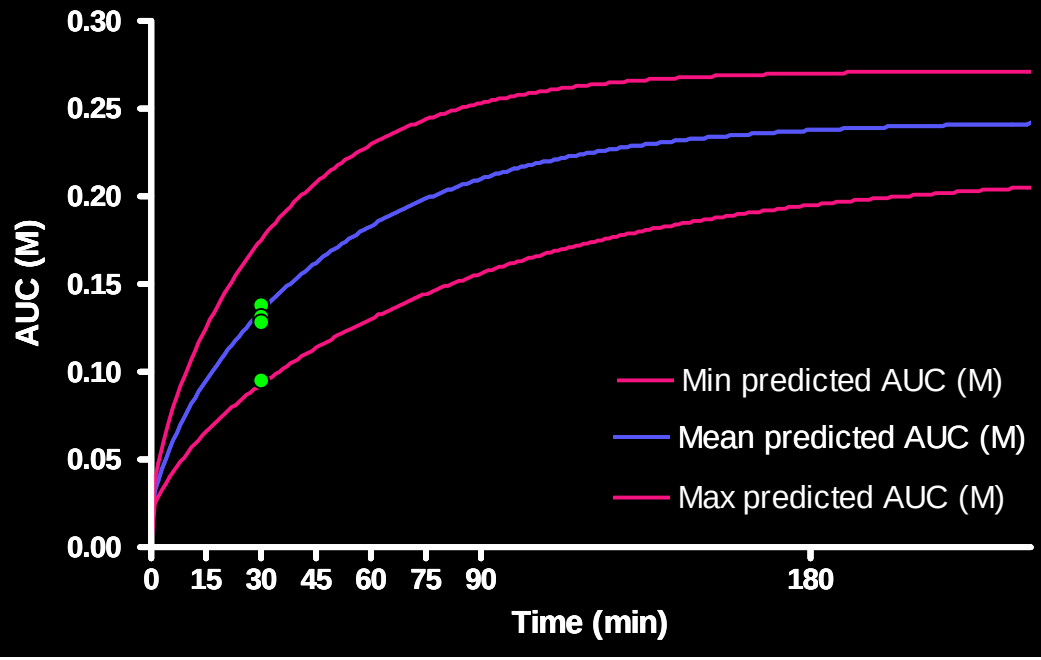

EXPERIMENTAL VALUES (n=7)

K = 2.8 ± 0.3

D/L^2 = 0.12 ± 0.05 h^{-1}

C. Herkenne et al., J. Invest. Dermatol., 127: 887-894(2007).

Fitting of data following application for 30 minutes yields estimates of transport parameters:

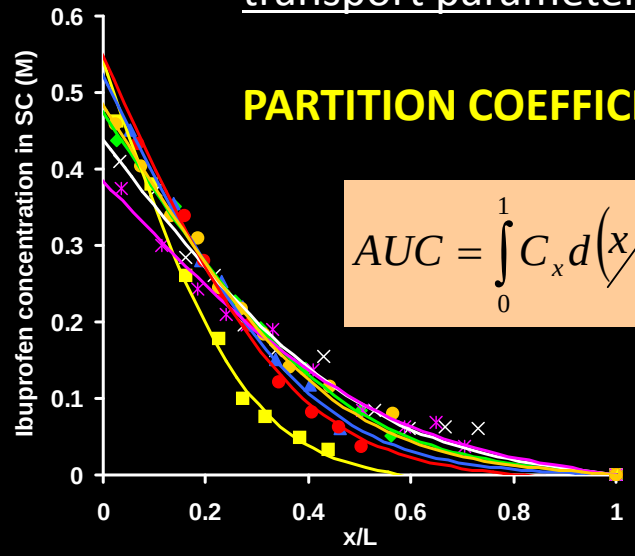

PARTITION COEFFICIENT, K

DIFFUSION PARAMETER, D/L^2

$$AUC = \int_0^1 C_x \, d\left(x/L\right) = K.C_v \left\{ \frac{1}{2} - \frac{4}{\pi^2} \sum_{n=0}^{\infty} \frac{1}{(2n+1)^2} \exp\left(- \frac{(2n+1)^2 . \pi^2 . D t}{L^2} \right) \right\}$$

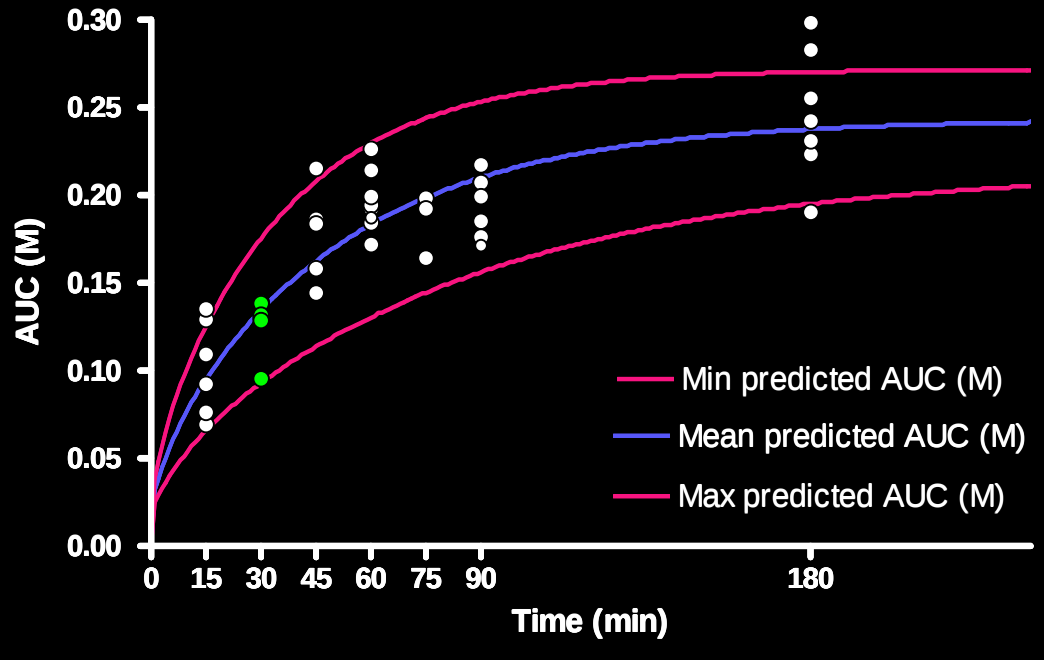

EXPERIMENTAL VALUES (n=7)

K = 2.8 ± 0.3

D/L^2 = 0.12 ± 0.05 h^{-1}

C. Herkenne et al., J. Invest. Dermatol., 127: 887-894(2007).

Coherent anti-Stokes Raman Scattering (CARS)

C. V. Raman
(Nobel Prize 1930)

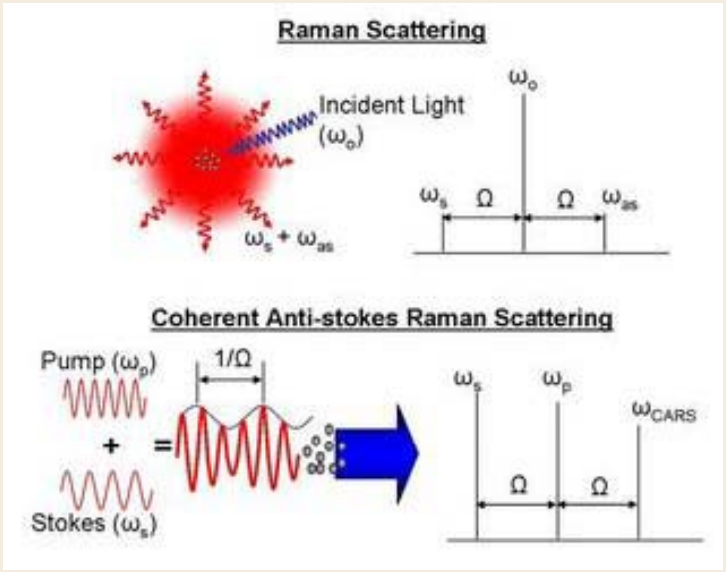

Pump-field is inelastically scattered off molecular vibrations of sample, generating new, red-shifted field components at the Stokes frequencies $\omega_s = \omega_0 - \Omega$

Unlike spontaneous Raman, CARS produces a highly directional field. Two excitation beams (ω_p and ω_s) form a beating field with frequency $\omega_p - \omega_s$.

When $\omega_p - \omega_s$ matches Ω, all molecules within the interaction volume vibrate in-phase.

http://newton.ex.ac.uk/research/biomedical/multiphoton/advantages/cars.html

Coherent Raman Scattering

ω_{pump}

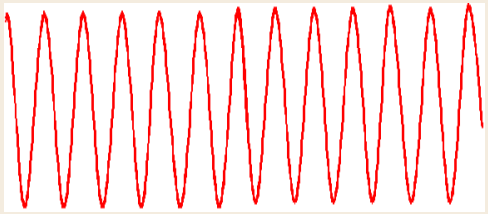

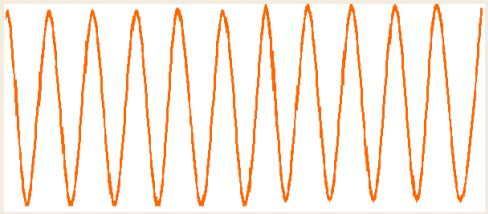

ω_{Stokes}

Beating at $\omega_{pump} - \omega_{Stokes}$

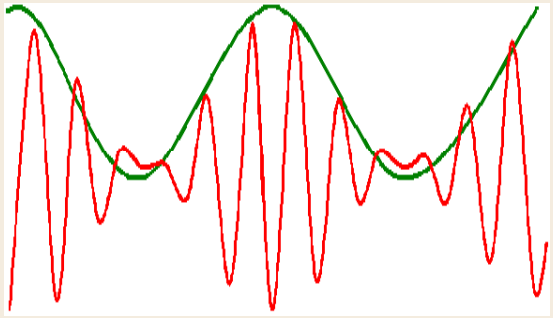

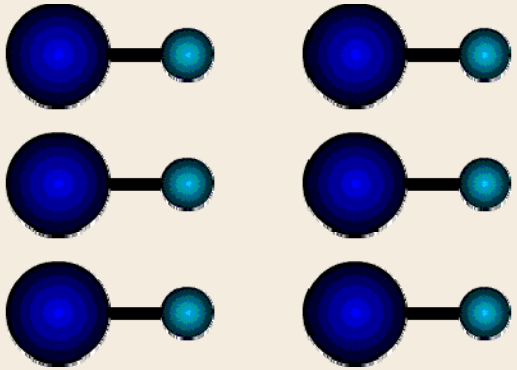

Stimulated excitation of coherent molecular vibration

$$\omega_{pump} - \omega_{Stokes} = \omega_{vib}$$

VOLUME 82, NUMBER 20 PHYSICAL REVIEW LETTERS 17 MAY 1999

Three-Dimensional Vibrational Imaging by Coherent Anti-Stokes Raman Scattering

Andreas Zumbusch,* Gary R. Holtom, and X. Sunney Xie†
Pacific Northwest National Laboratory, William R. Wiley Environmental Molecular Sciences Laboratory, P.O. Box 999, K8-88, Richland, Washington 99352
(Received 9 December 1998)

A multiphoton microscopy based on coherent anti-Stokes Raman scattering is accomplished with near-infrared ultrashort laser pulses. We demonstrate vibrational imaging of chemical and biological samples with high sensitivity, high spatial resolution, noninvasiveness, and three-dimensional sectioning capability. [S0031-9007(99)09110-3]

Coherent Raman imaging

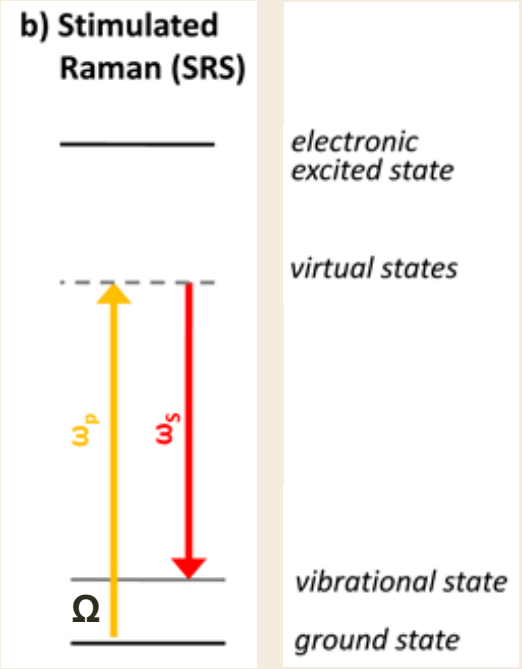

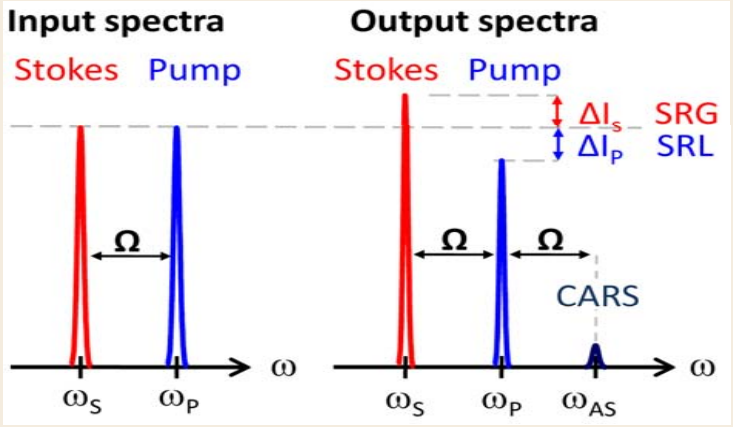

Stimulated Raman Scattering (SRS) microscopy

Both pump- and Stokes-frequencies are incident on sample.

If frequency difference $\Delta\omega = \omega_p - \omega_S$ matches a molecular vibration of sample Ω, stimulated excitation of vibration transitions occurs.

Intensity of pump-field experiences a loss (SRL) and the Stokes field a gain (SRG).

SRS -> intensity increase in Stokes beam (SRG) and a decrease in pump beam (SRL). **[Also shown (not to scale) is CARS signal generated at anti-Stokes frequency]**

Stimulated Raman scattering

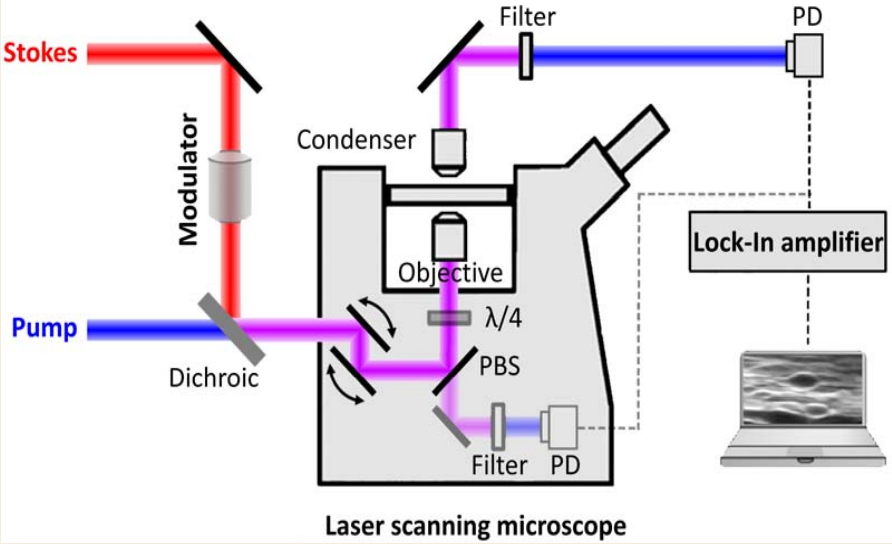

* Stokes beam provided by 1064 nm pulsed laser
* Pump beam by a synchronously-pumped optical parametric oscillator
* Intensity of Stokes beam modulated at radio-frequency.
* Pump- and Stokes beams are overlapped in time and space and aligned into laser–scanning microscope

In forward and epi-direction, Stokes beam is blocked and pump beam detected with large-area photodiode

SRS signal extracted with lock-in amplifier detecting at same frequency of modulation of Stokes beam

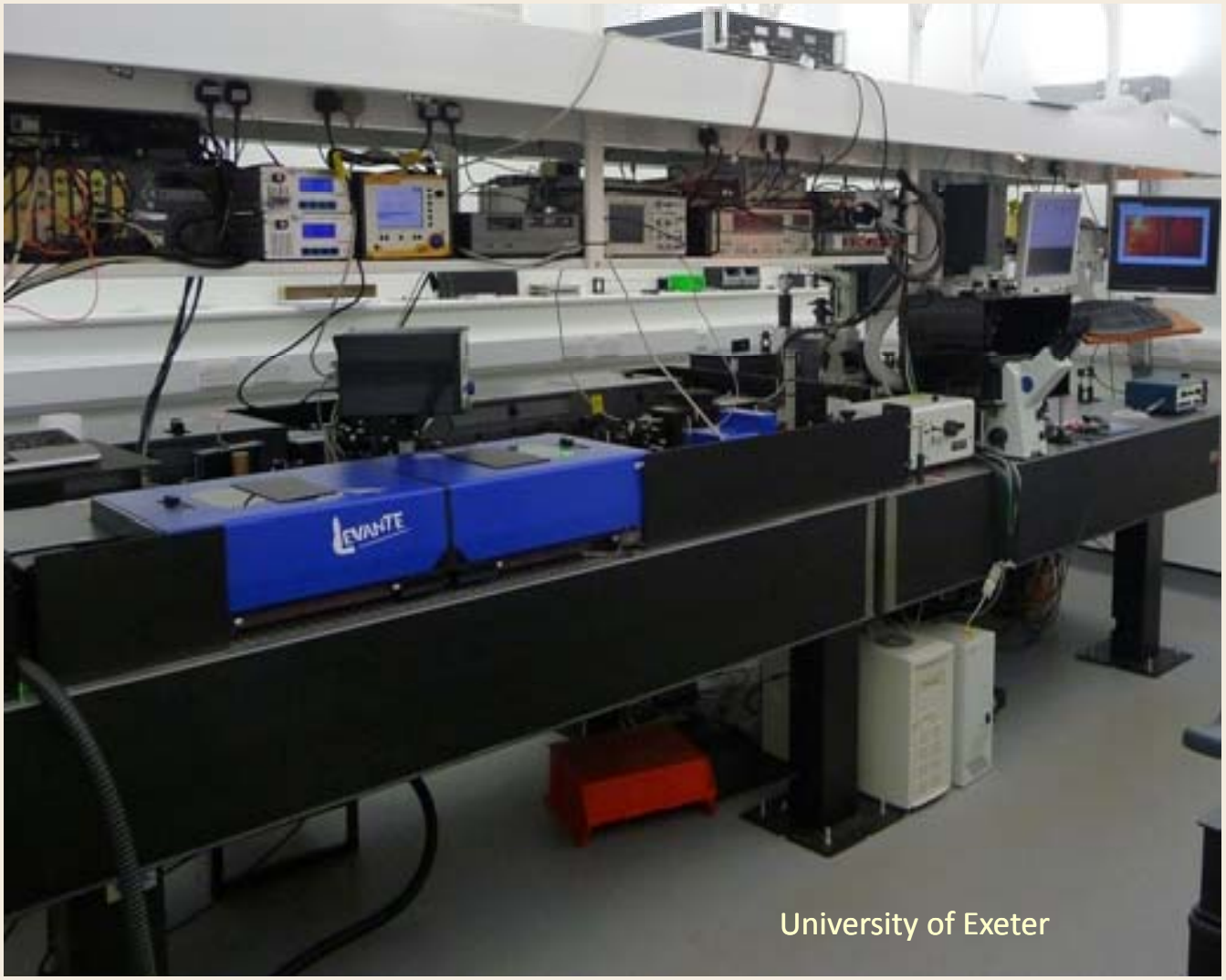

University of Exeter

Advantages of CRS

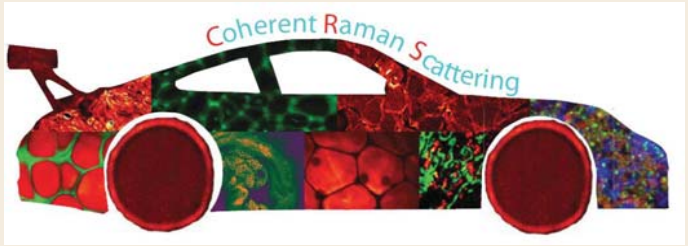

- Raman resonance enhancement provides chemical selectivity without need for labelling.
- There is little scattering of the near-infrared excitation beams, allowing deep penetration in tissues.
- Due to anti-Stokes shift, CARS signal is of shorter wavelength than one-photon fluorescence.
  - allows detection in presence of a strong fluorescent background.
- Coherent addition of CARS fields generates a large signal.
- Nonlinear dependence on excitation intensities -> inherent 3D resolution.
- Low absorption of near-infrared excitation beams significantly reduces photodamage in biological samples.

http://newton.ex.ac.uk/research/biomedical/multiphoton/advantages/cars.html

CARS ➡ SRS

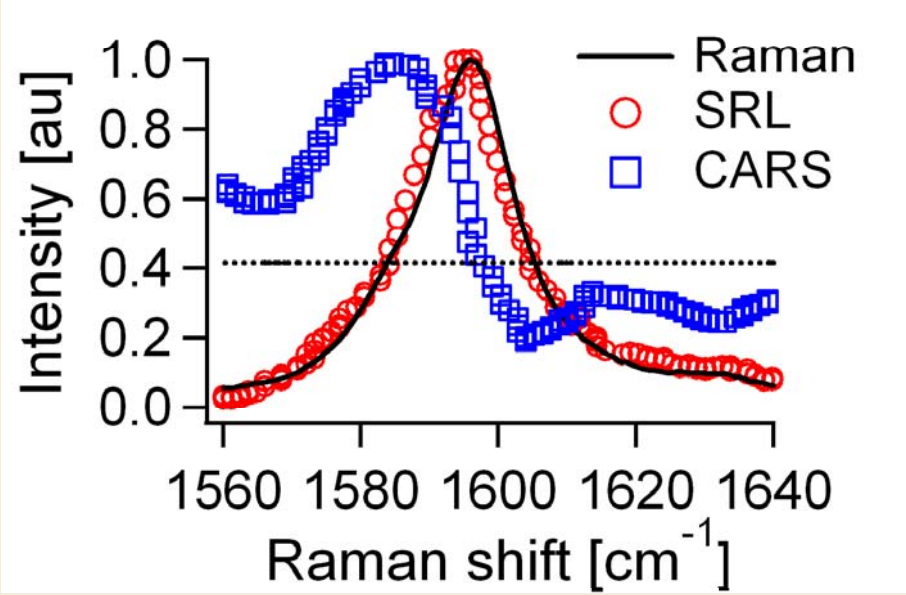

***trans*-retinol in EtOH**

No non-resonant background

No spectral distortion; SRS spectra identical to spontaneous Raman

Ready spectroscopic identification base in Raman literature

Capable of imaging in the crowded fingerprint region

SRS: linear concentration dependence

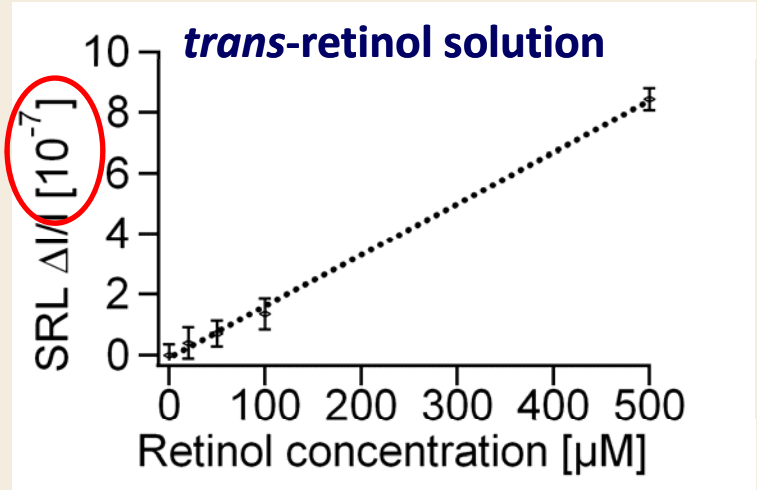

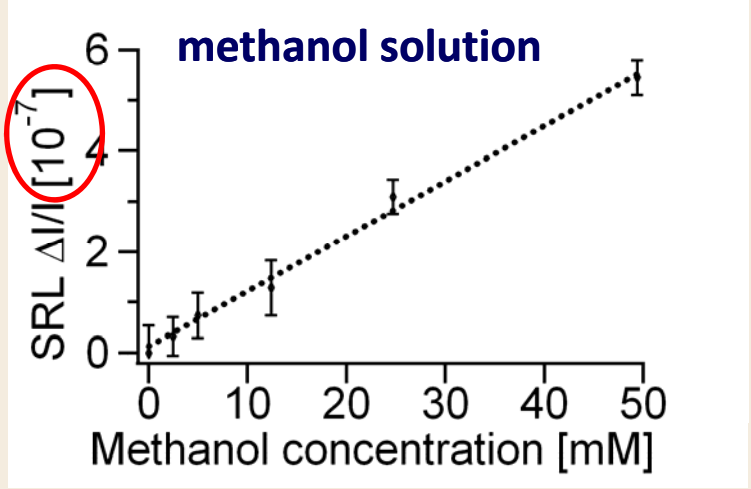

- **SRL signal is linear in concentration (easy quantification)**
- **Sensitivity limits: Retinol 50 μM (3000 oscillators in focus)**
  Methanol 5 mM (3x10^5 oscillators in focus)

SRS is more sensitive than CARS

Imaging Lipids in *C. Elegans*

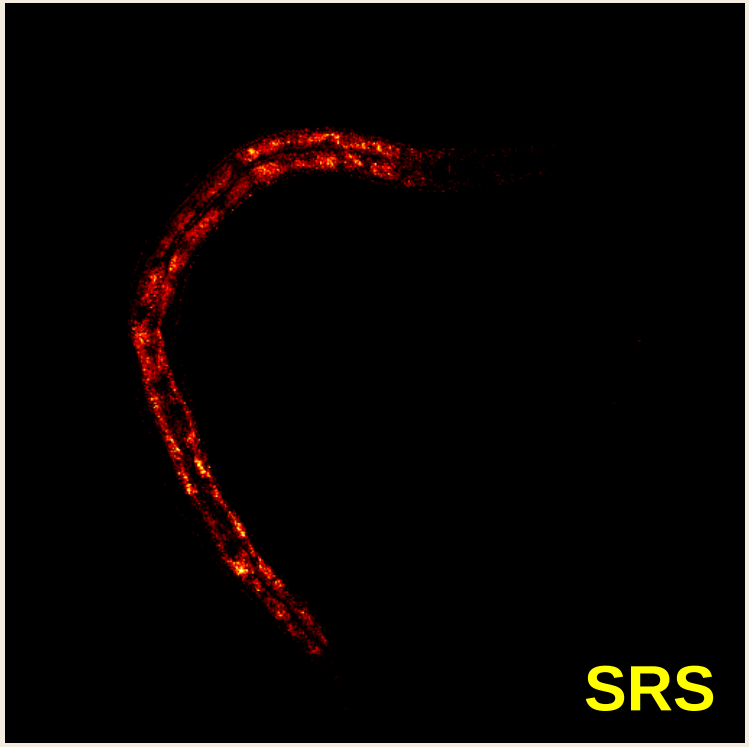

@2845 cm^{-1} CH_2 stretching

Wang et al. *Nature Methods* (2011)

SRS images from various organs

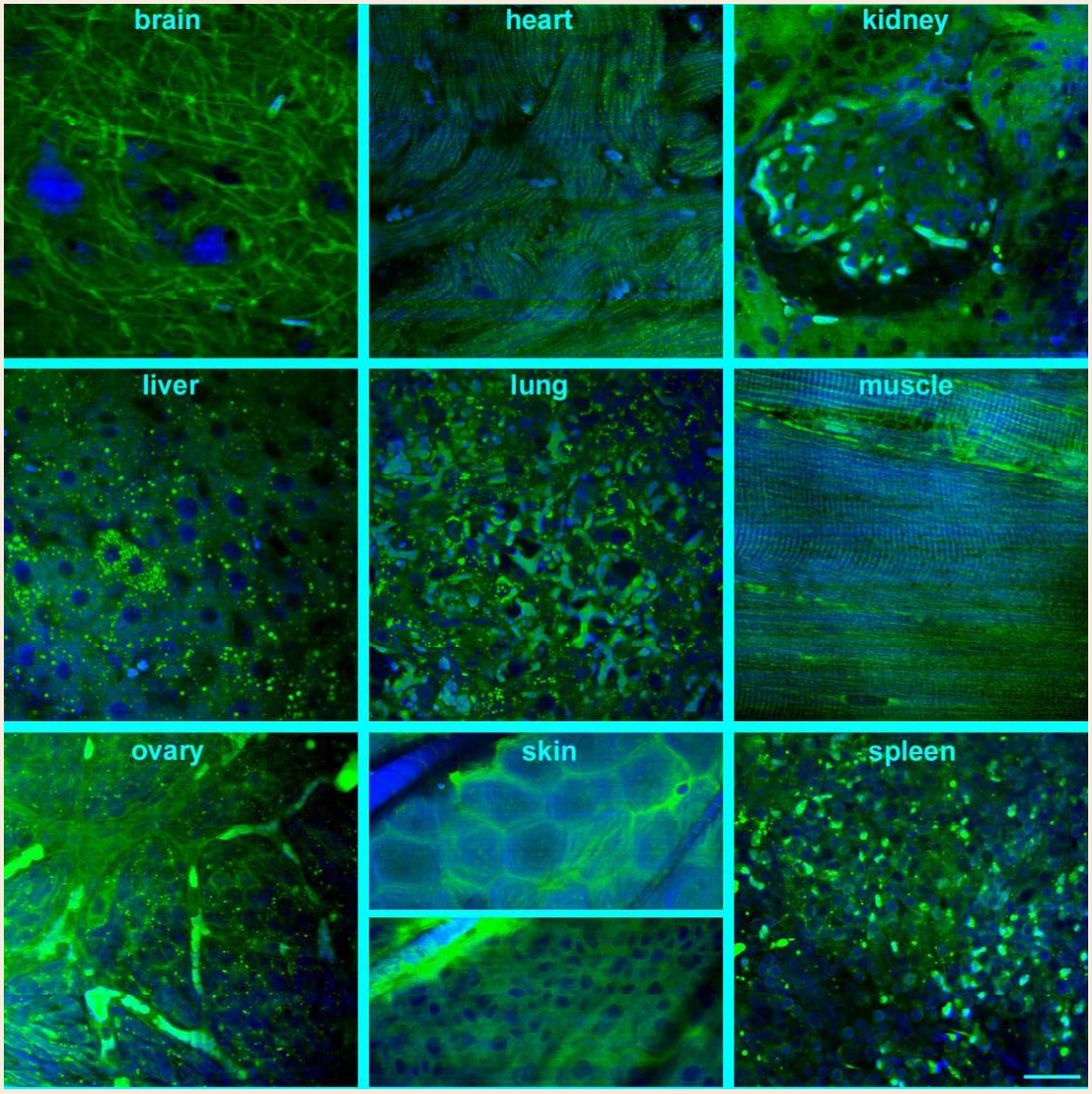

Chemical contrast of sebaceous glands

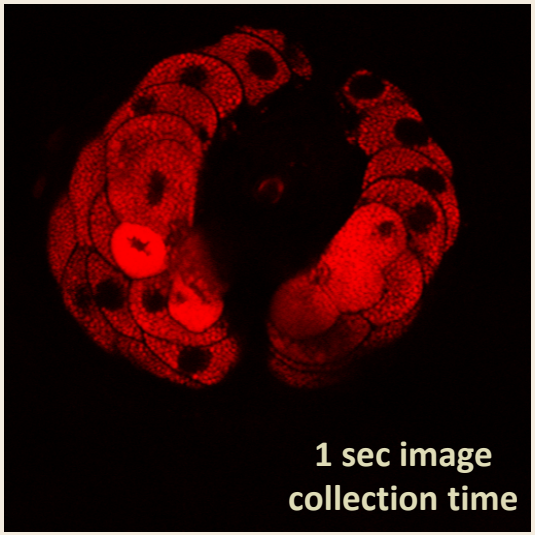

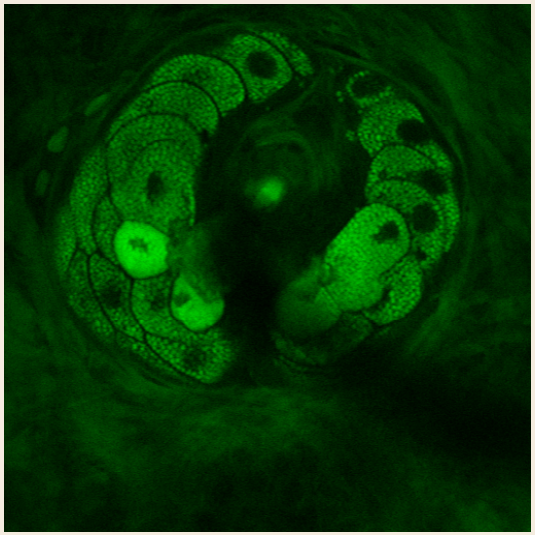

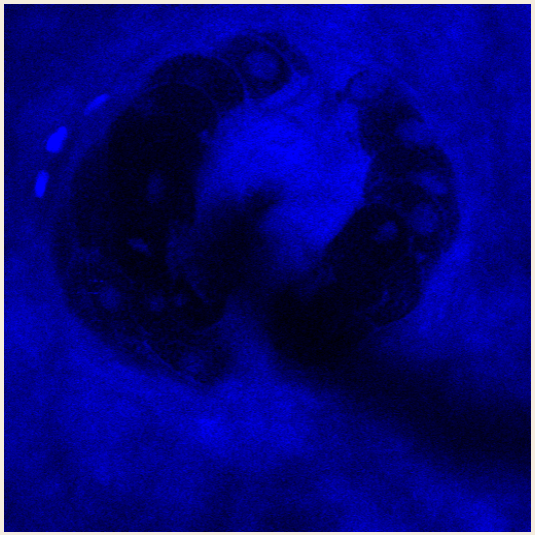

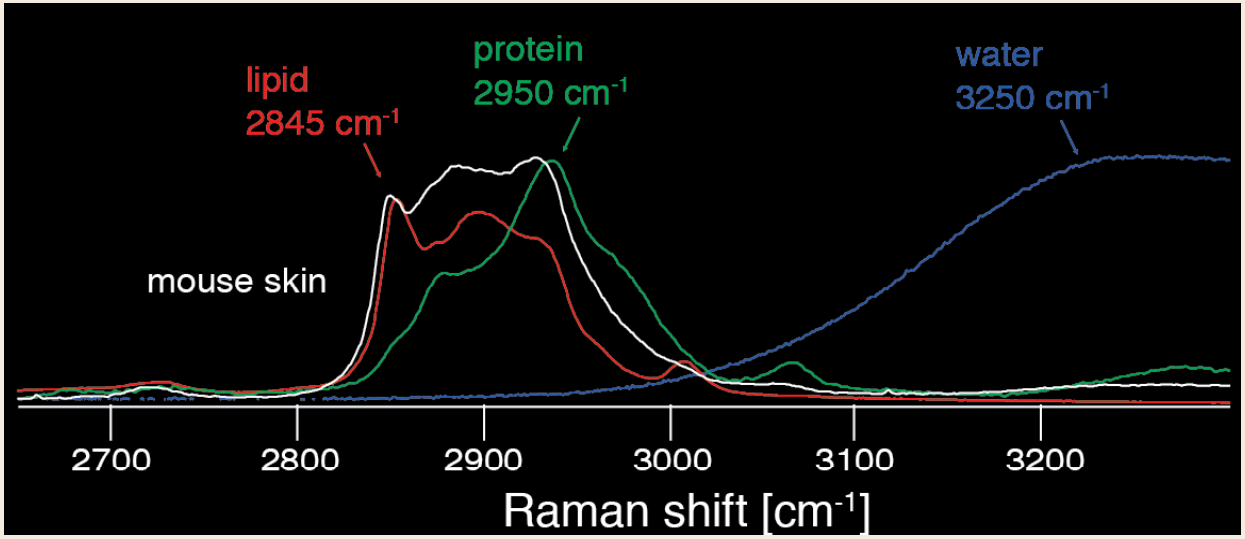

Video rate SRS imaging of mouse ear skin

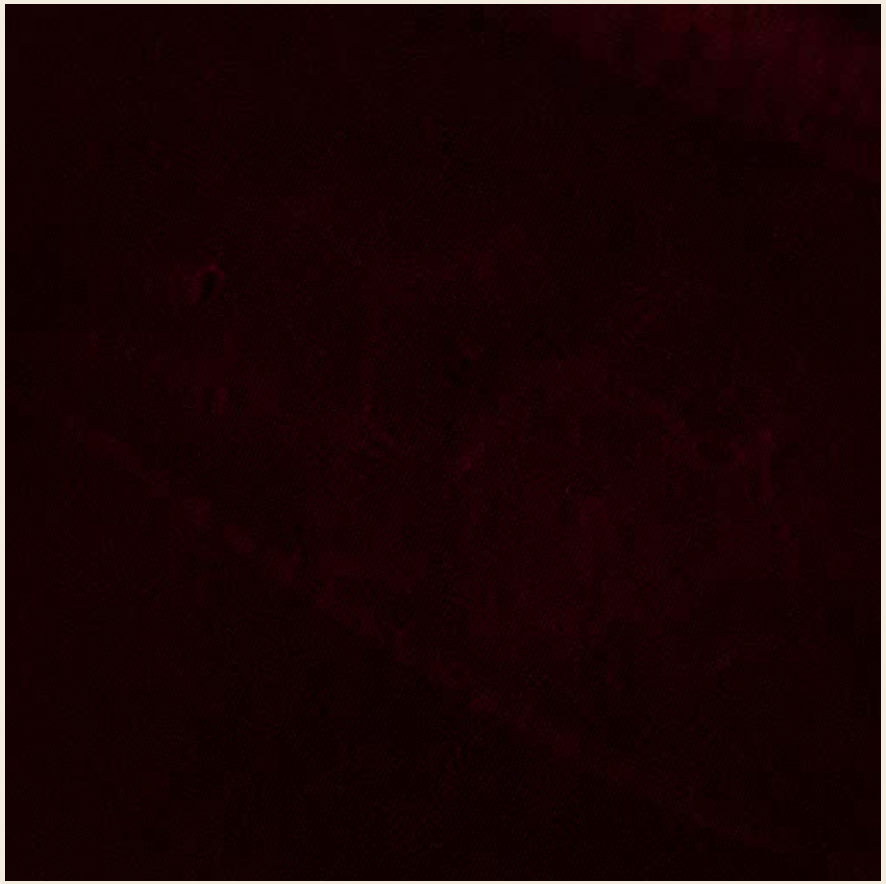

SRS CH_2 images of mouse skin at 2846 cm^{-1}

Saar et al., Science, 330, 1368 (2010)

SRS CH_2 images of mouse ear skin at 2846 cm^{-1}

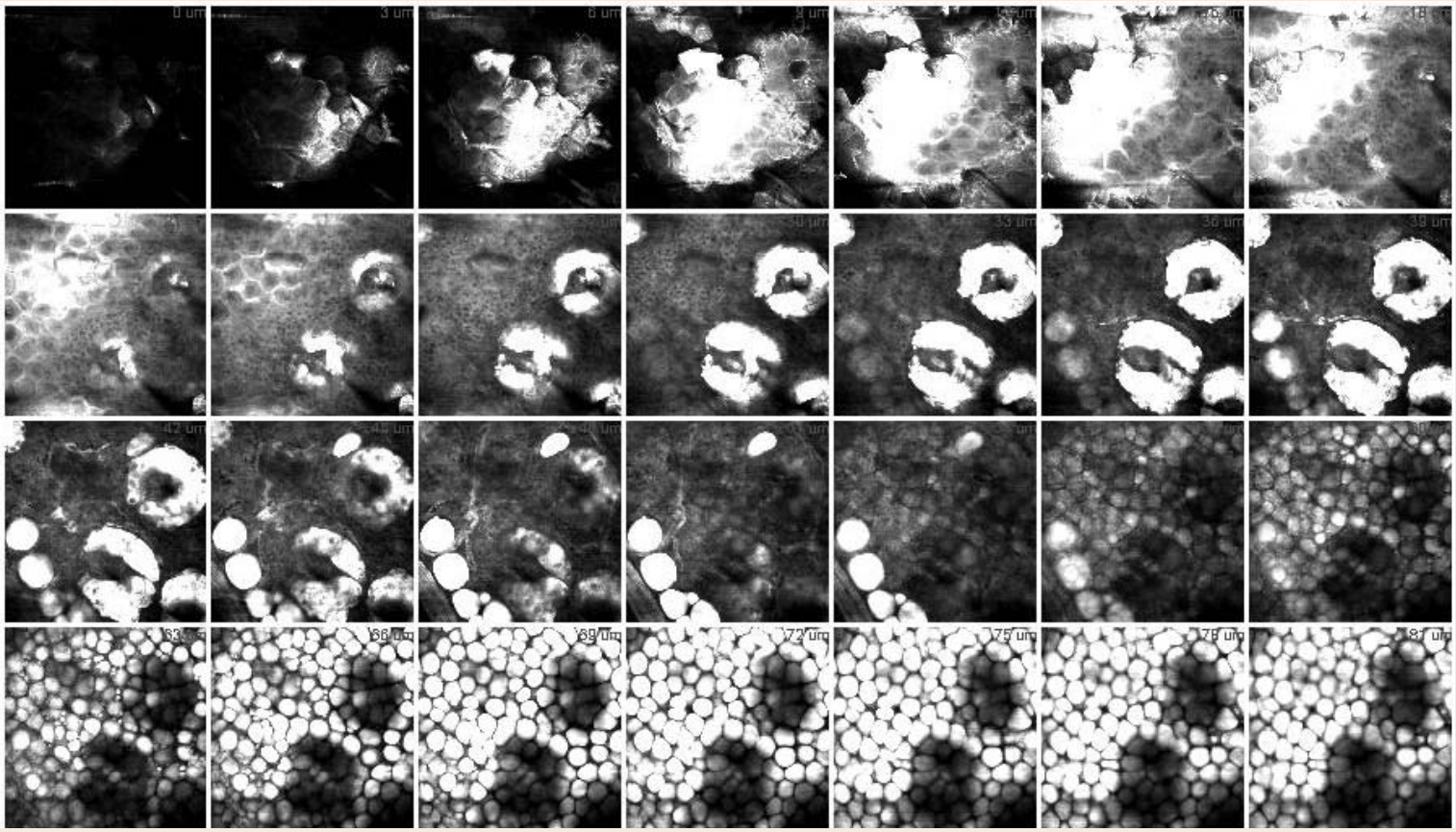

BG Saar, LR Contreras-Rojas, XS Xie, RH Guy, Molecular Pharmaceutics 8, 969-975 (2011)

SRS CH_2 images of mouse ear skin at 2846 cm^{-1}

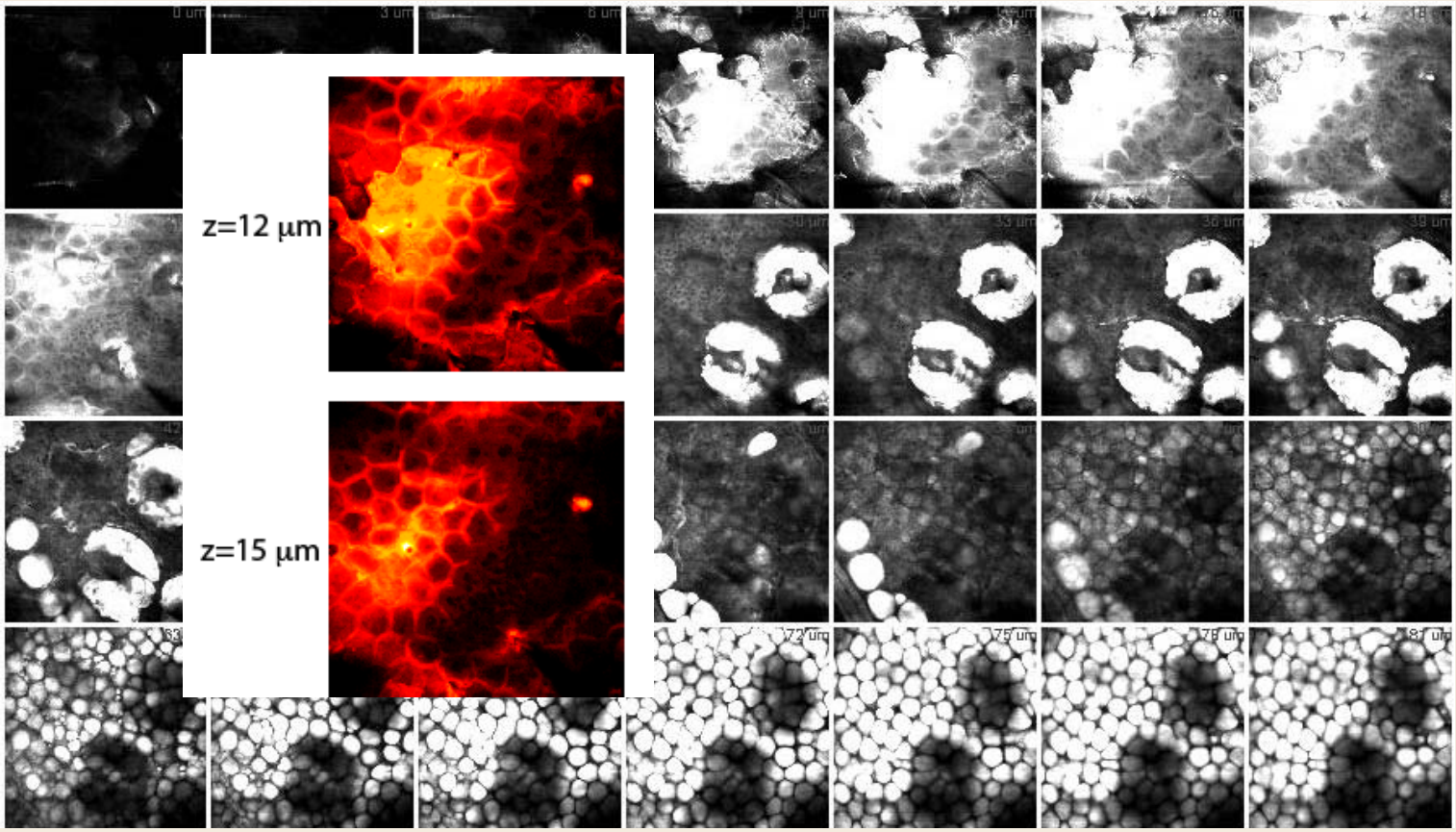

BG Saar, LR Contreras-Rojas, XS Xie, RH Guy, Molecular Pharmaceutics 8, 969-975 (2011)

Raman spectra of key chemical species

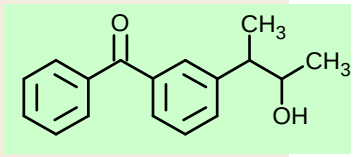

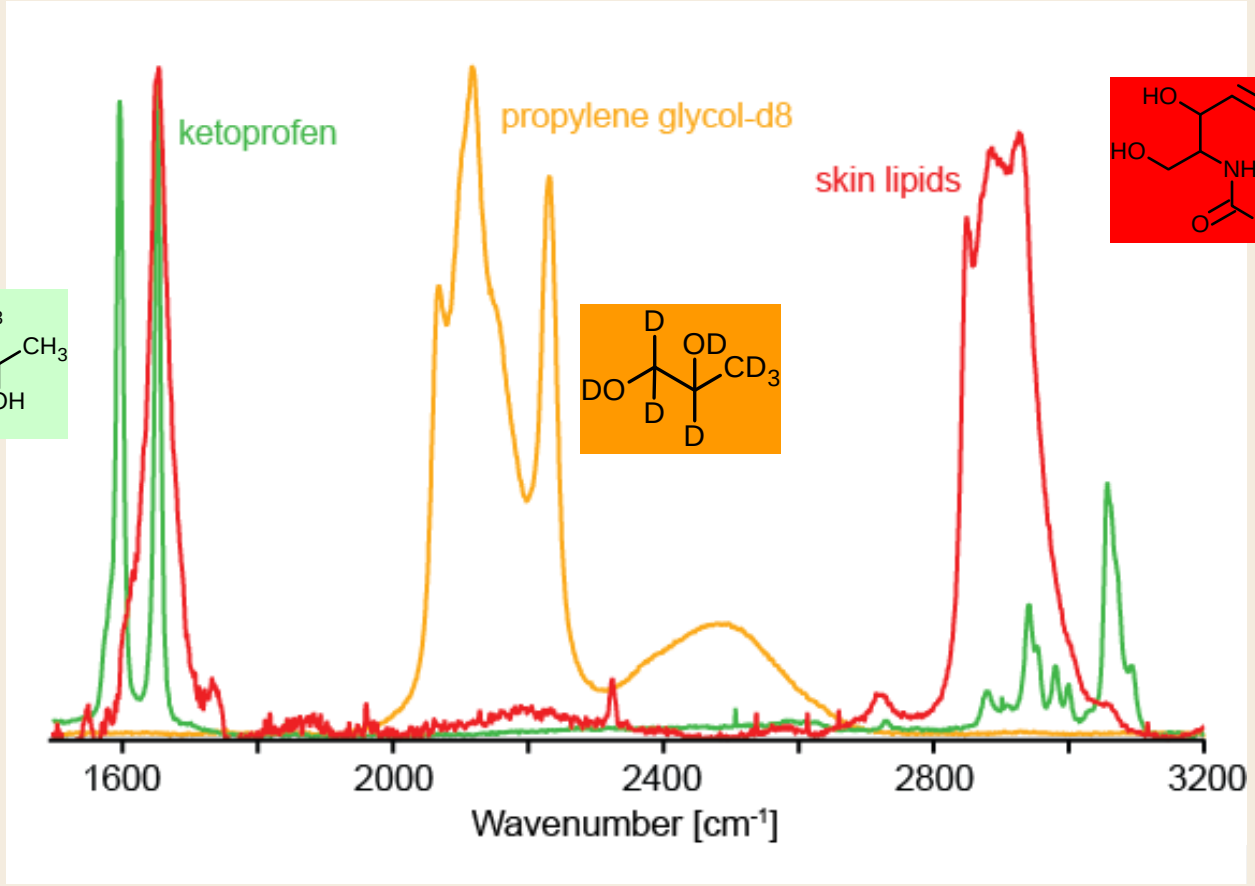

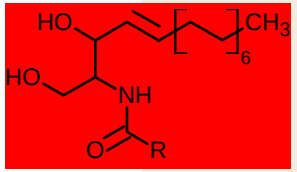

SRS contrast is based on spontaneous Raman spectra, which are used to determine optimal excitation wavelengths: 1599 cm^{-1}, 2120 cm^{-1} and 2845 cm^{-1} report on ketoprofen, deuterated PG and skin lipids, respectively.

Diffusion of deuterated PG across skin

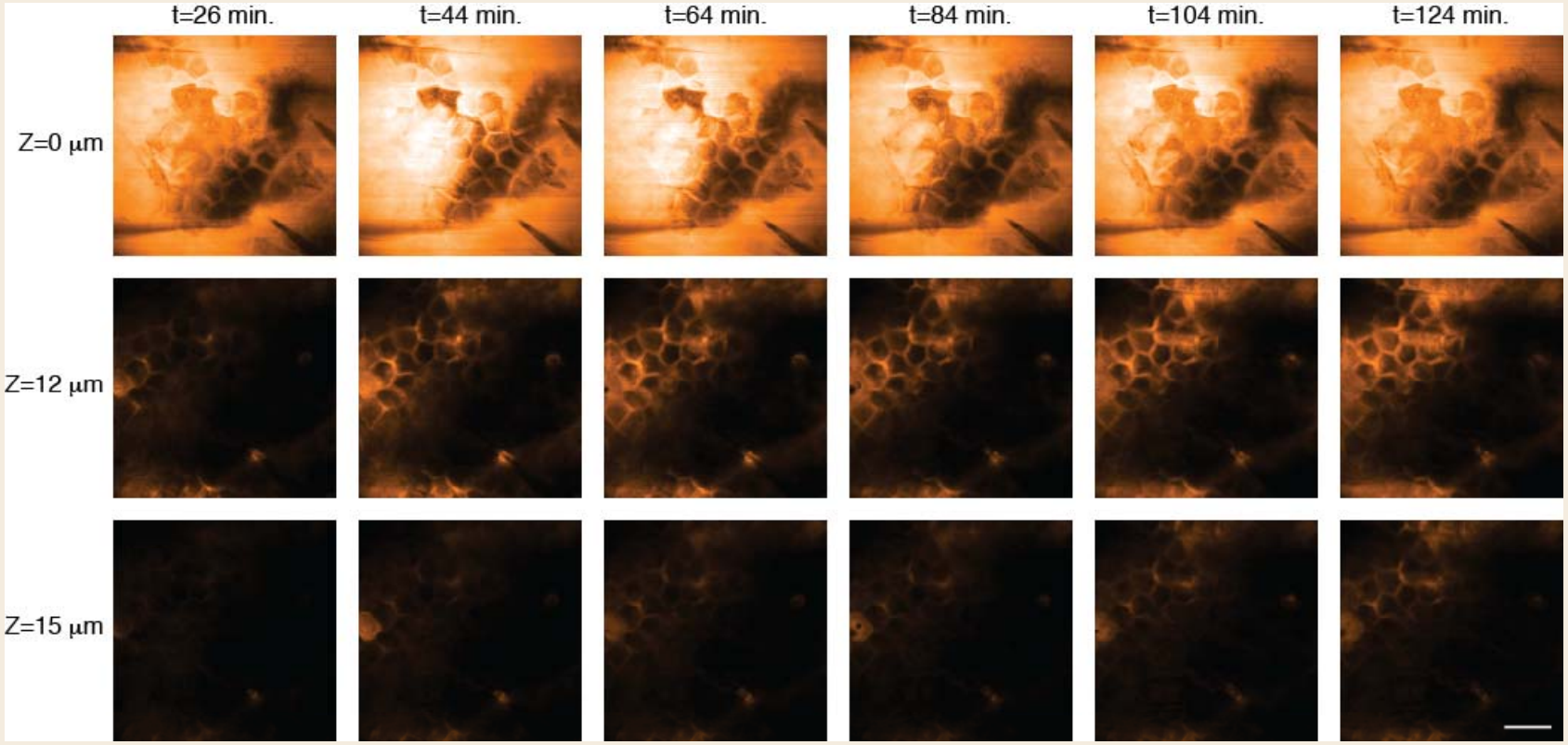

BG Saar, LR Contreras-Rojas, XS Xie, RH Guy, Molecular Pharmaceutics 8, 969-975 (2011)

Diffusion of ketoprofen across skin

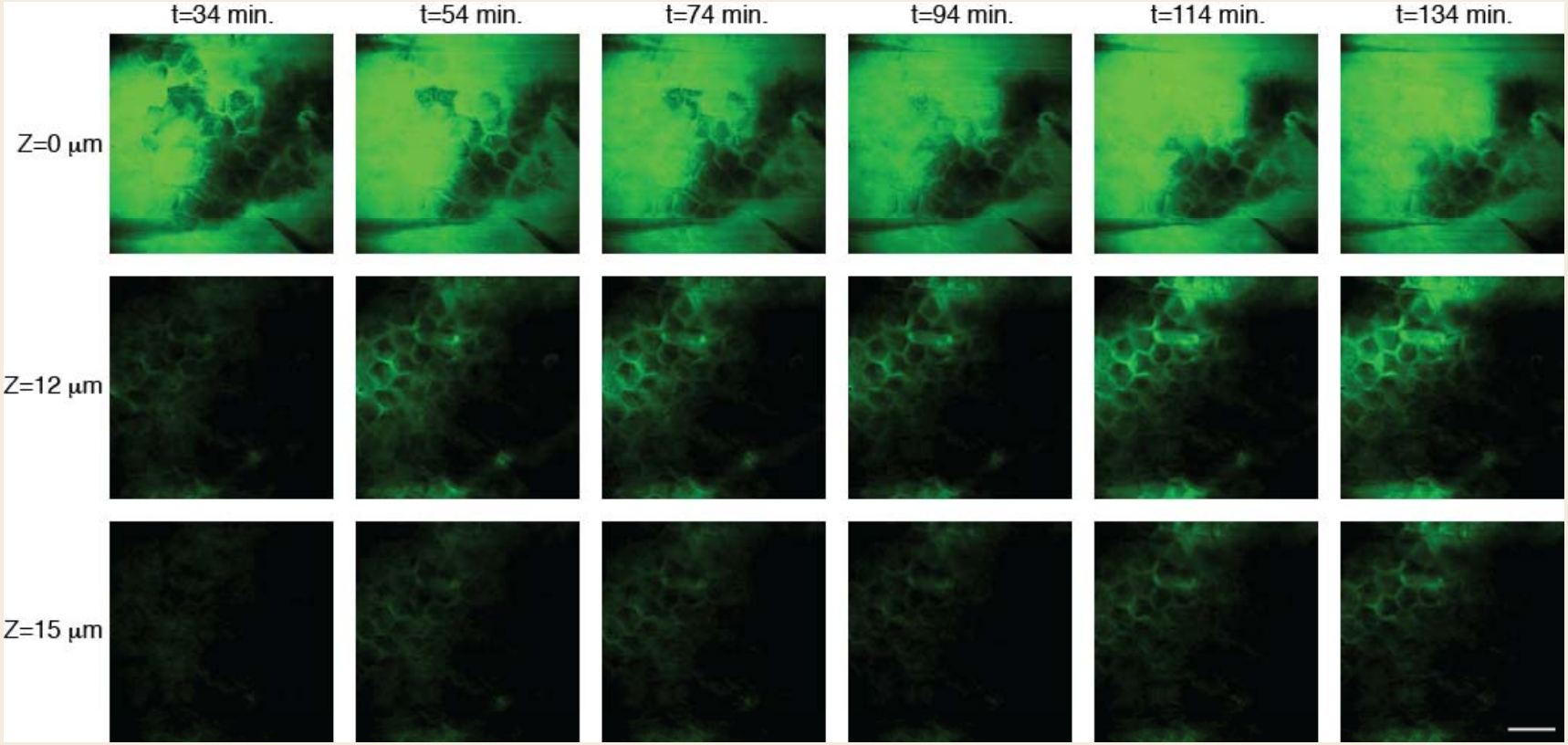

BG Saar, LR Contreras-Rojas, XS Xie, RH Guy, Molecular Pharmaceutics 8, 969-975 (2011)

SRS analysis of skin penetration pathways

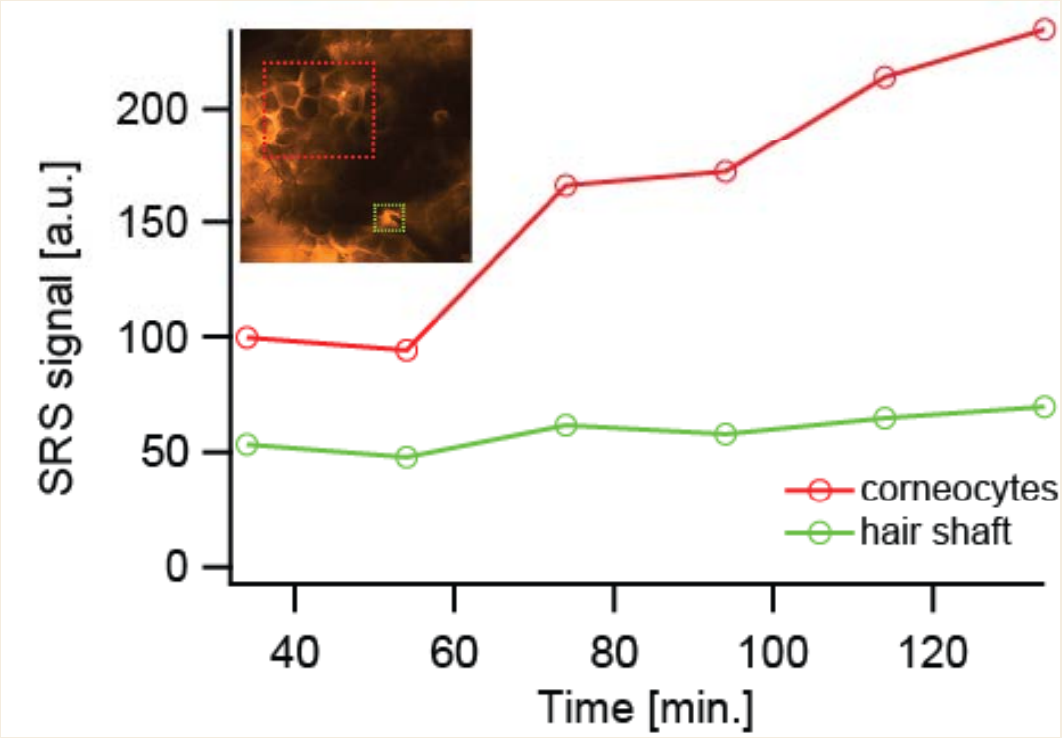

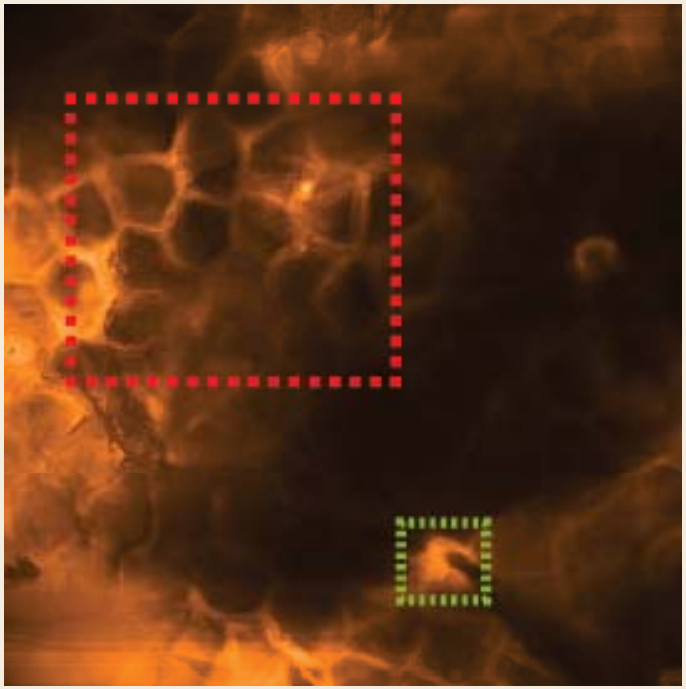

* **Temporal profiles of PG-d8 at z = 6 µm from two distinct regions**
* **Intercellular penetration increases steadily with time**
* **Follicular transport already 'saturated' at 26 mins post-application**
* **Scheuplein was right!**

BG Saar, LR Contreras-Rojas, XS Xie, RH Guy, Molecular Pharmaceutics 8, 969-975 (2011)

Depth-profiling analysis of skin penetration

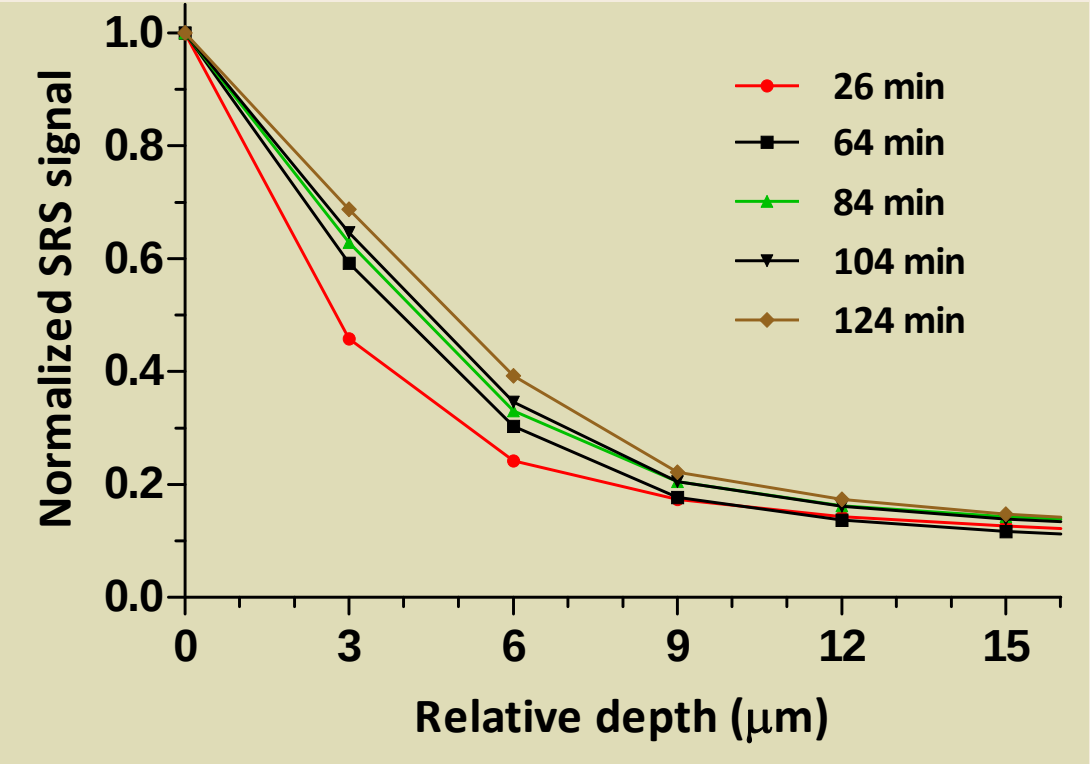

* Depth profiles of PG-d8 as a function of time
* Experimental measurements from integration of SRS signal
* Location of skin surface is approximate

BG Saar, LR Contreras-Rojas, XS Xie, RH Guy, Molecular Pharmaceutics 8, 969-975 (2011)

Depth-profiling analysis of skin penetration

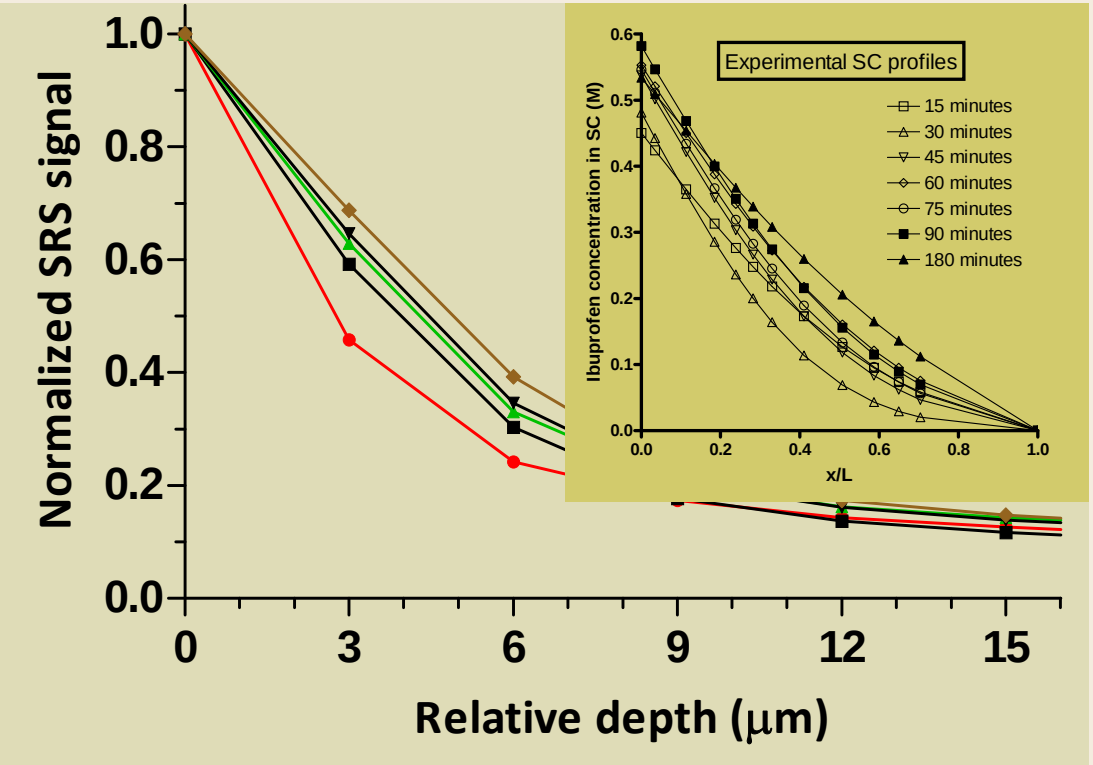

* Depth profiles of PG-d8 as a function of time
* Experimental measurements from integration of SRS signal
* Location of skin surface is approximate

Depth-profiling analysis of skin penetration

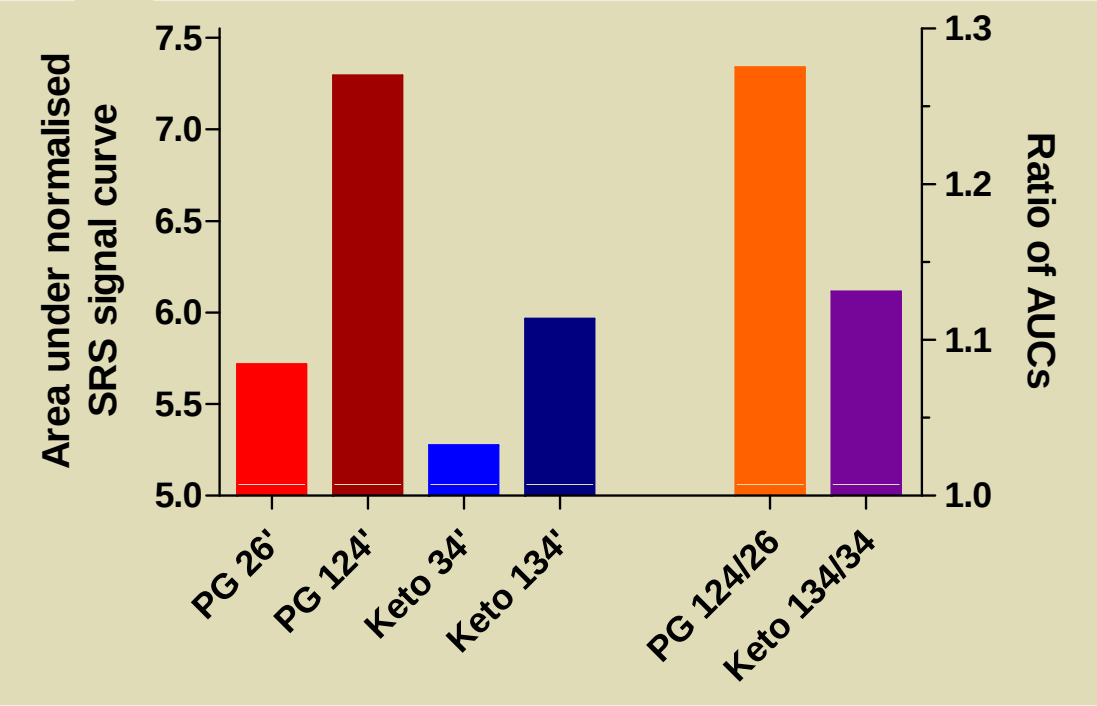

* Comparison of relative penetration of PG-d8 and ketprofen over the course of the experiment (~2 hr) [left-hand axis]
* Ratio of AUCs (measured near the beginning and end of the exposure) indicate faster permeation of PG relative to ketoprofen [right-hand axis]

BG Saar, LR Contreras-Rojas, XS Xie, RH Guy, Molecular Pharmaceutics 8, 969-975 (2011)

Metamorphosis of a formulation

Ibuprofen-d3 dissolved in propylene glycol at close to saturation

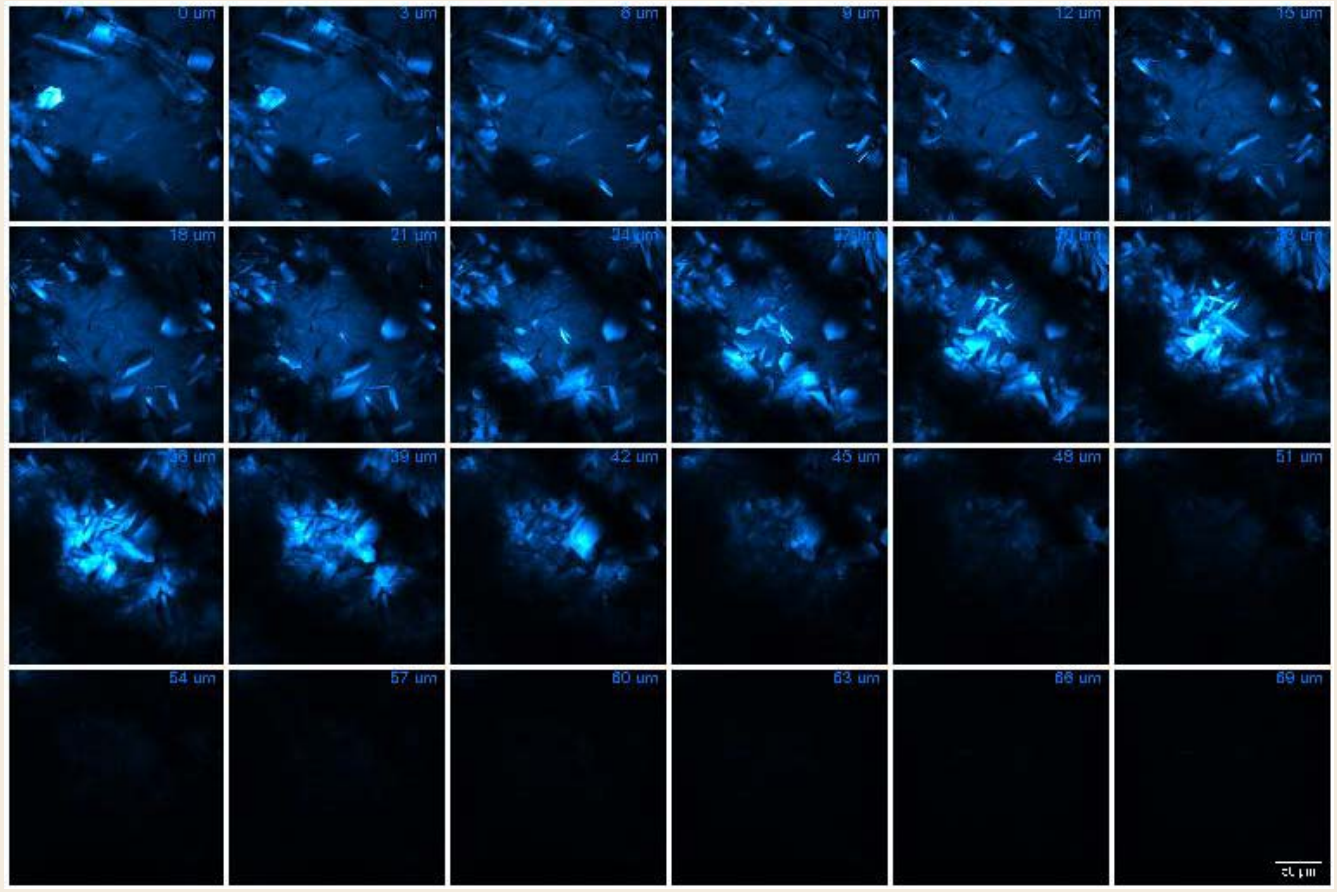

BG Saar, LR Contreras-Rojas, XS Xie, RH Guy, Molecular Pharmaceutics 8, 969-975 (2011)

Metamorphosis of a formulation

Ibuprofen-d3 dissolved in propylene glycol at close to saturation

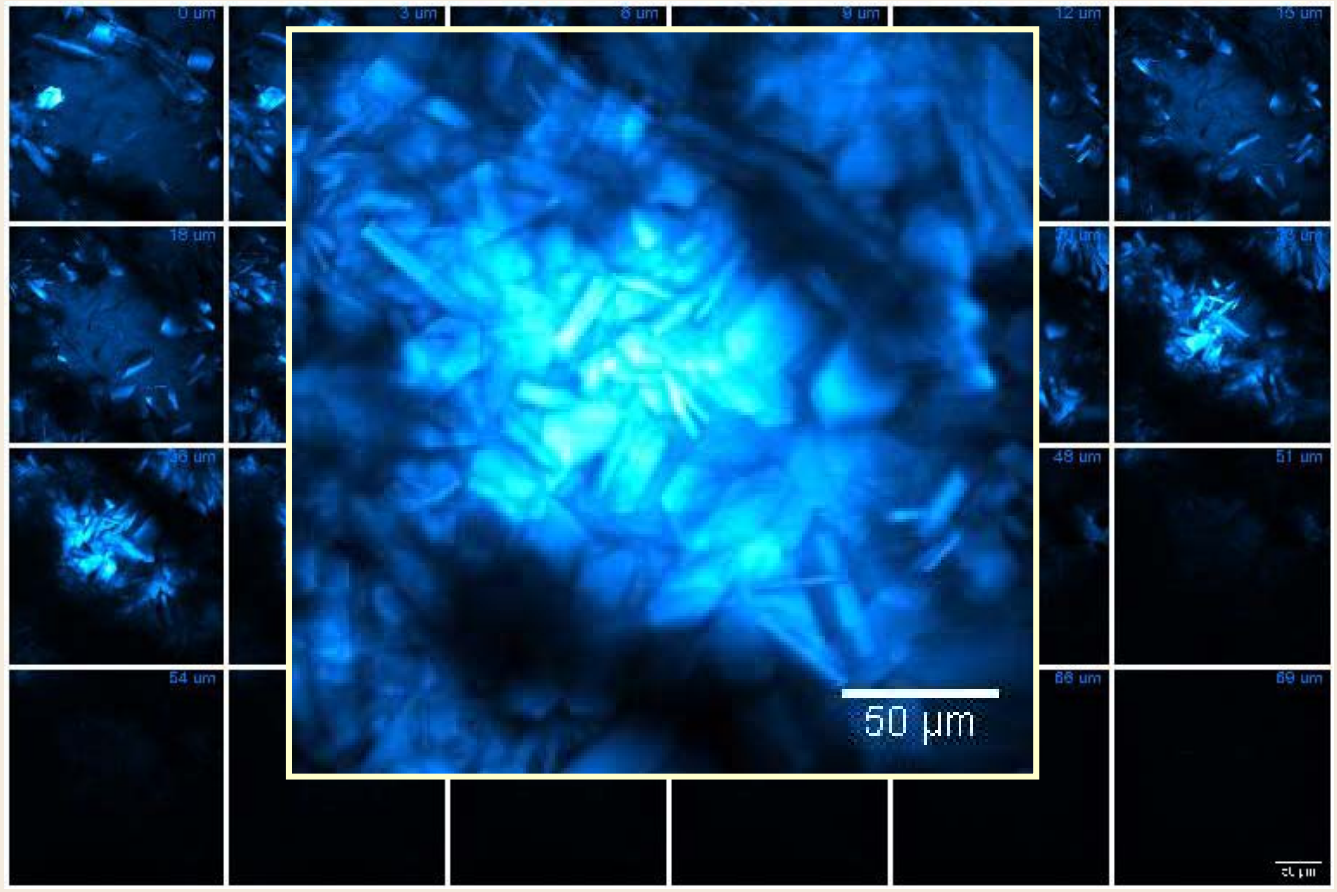

BG Saar, LR Contreras-Rojas, XS Xie, RH Guy, Molecular Pharmaceutics 8, 969-975 (2011)

Epi-detection of back-scattered light

Annular photodiode

Detecting 30% incident light allowing video rate epi-SRS

Blocking filter

Cover slip

Tissue

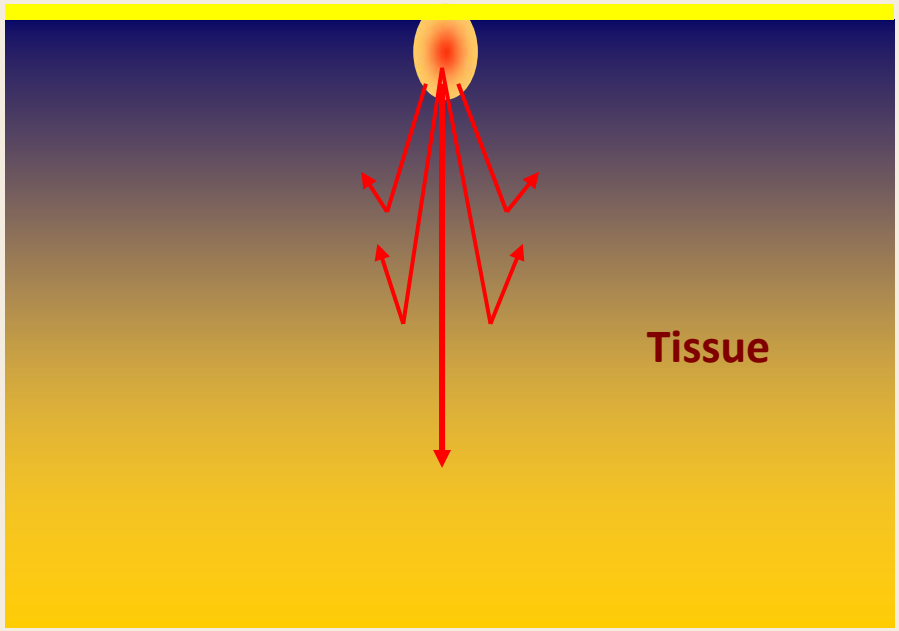

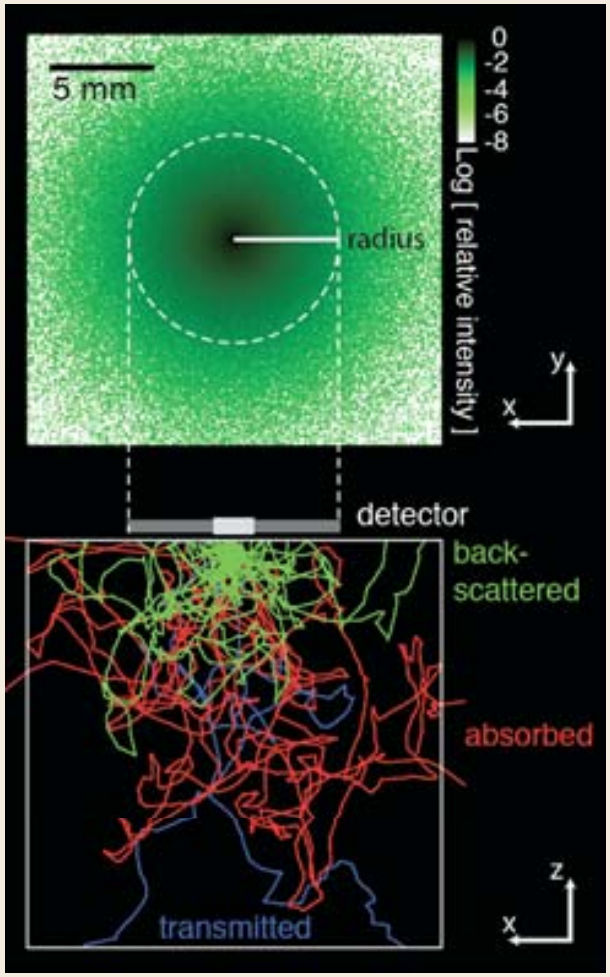

Saar et al. *Science,* 330, 1368 (2010)

Fast SRS imaging in vivo

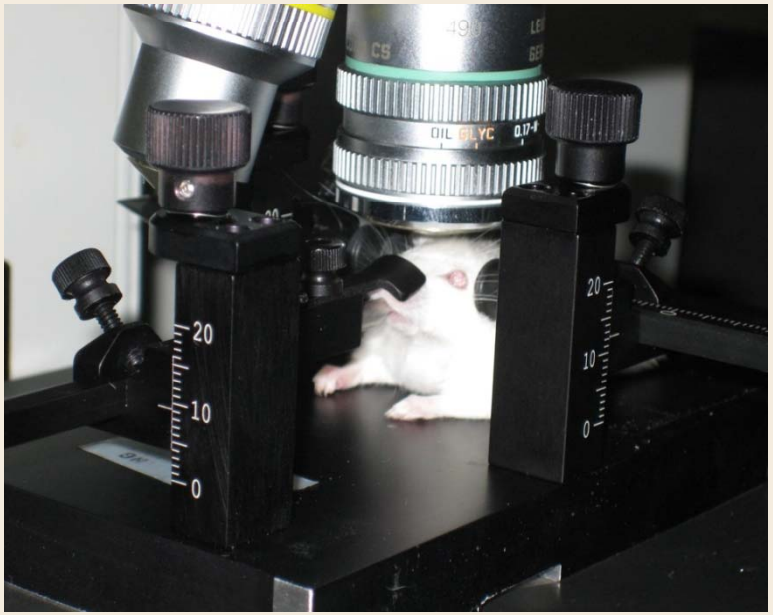

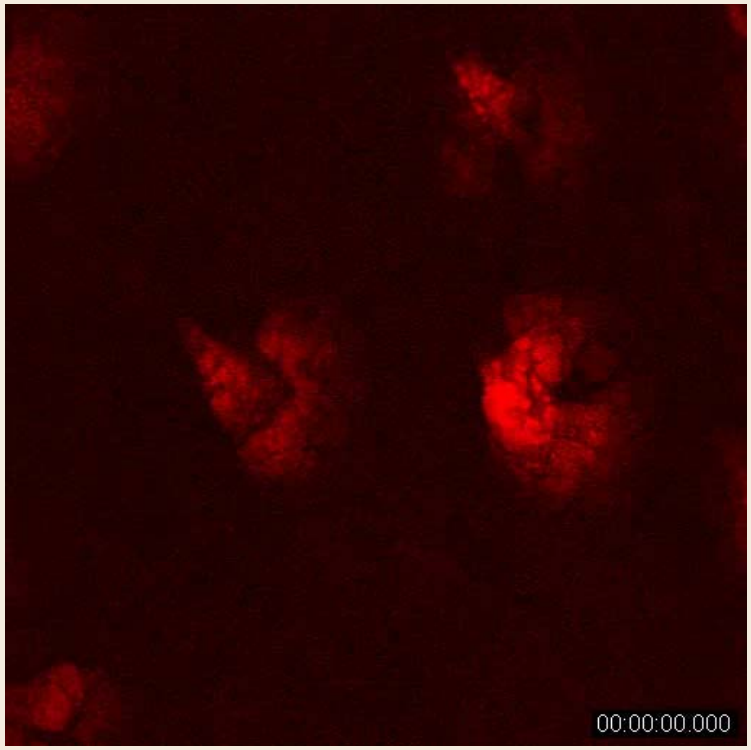

Saar et al. *Science,* 330, 1368 (2010)

Sebaceous gland at 2845 cm^{-1}
40 µm into mouse skin

In Vivo Video Rate Imaging: Human Volunteer with a Leica Microscope

CH_3 images (protein contrast) 2950 cm^{-1}

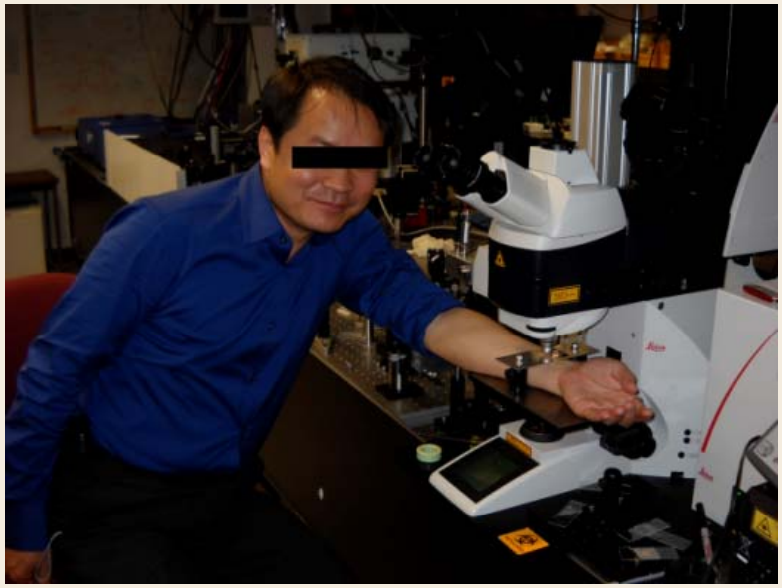

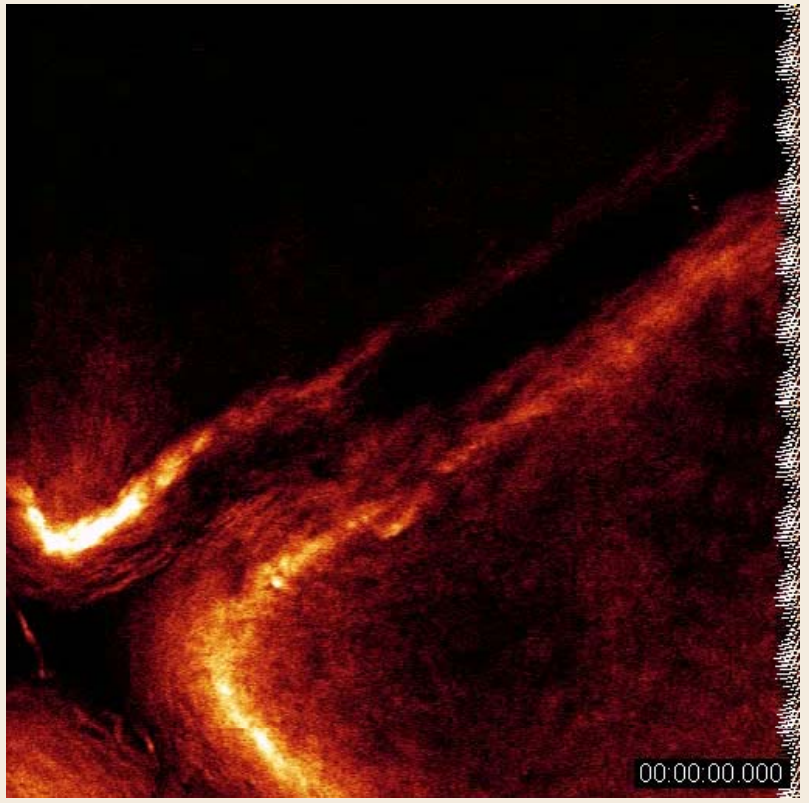

Saar et al. *Science,* 330, 1368 (2010)

Conclusions

- **Selecting topical/transdermal drug candidates must consider both potency and skin permeability.**
  - **Lipinski's rules are not irrelevant to skin.**

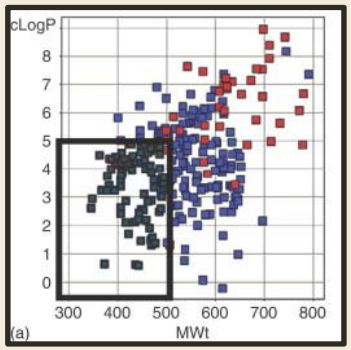

- **Novel, non-invasive imaging techniques may (semi-) quantify drug delivery into and through skin.**
  - **"metamorphosis" of formulations post-application**
  - **potential to improve topical formulations and optimise drug bioavailability.**

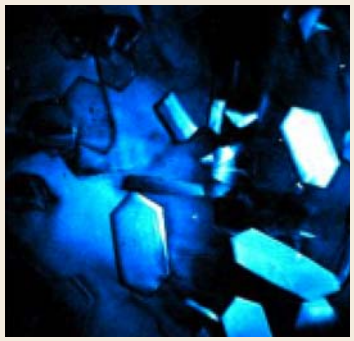

- **Uptake of chemicals across skin is primarily governed by physical laws**
  - **more complex models have not revealed commensurate insight**